KU LEUVEN

FACULTEIT GENEESKUNDE
BIOMEDISCHE WETENSCHAPPEN

Opbouw en karakterisatie van een nieuw ziektemodel voor Multipele Systeem Atrofie gebaseerd op virale vectoren in ratten

Generation and characterization of a novel viral vector-based disease model for Multiple System Atrophy in rats

Masterproef voorgedragen tot het behalen van de graad van Master in de biomedische wetenschappen door

Nathalie JACOBS

Promotor: Prof. dr. Veerle BAEKELANDT
Begeleider: Filipa BRITO
Departement Neurowetenschappen
Onderzoeksgroep Neurobiologie en Gentherapie

Leuven, 2018-2019

KU LEUVEN

FACULTEIT GENEESKUNDE
BIOMEDISCHE WETENSCHAPPEN

Opbouw en karakterisatie van een nieuw ziektemodel voor Multipele Systeem Atrofie gebaseerd op virale vectoren in ratten

Generation and characterization of a novel viral vector-based disease model for Multiple System Atrophy in rats

Masterproef voorgedragen tot het behalen van de graad van Master in de biomedische wetenschappen door

Nathalie JACOBS

Promotor: Prof. dr. Veerle BAEKELANDT
Begeleider: Filipa BRITO
Departement Neurowetenschappen
Onderzoeksgroep Neurobiologie en Gentherapie

Leuven, 2018-2019

PREFACE

First of all, I would like to thank my promotor Prof. dr. Veerle Baekelandt for giving me the opportunity of doing my Master's thesis in the Laboratory for Neurobiology and Gene Therapy, and for giving me her guidance and support during this project. I would also like to thank my daily supervisor Filipa Brito, for everything she has taught me during this year. I learned a lot of scientific skills and gained insight into this research field because of her. I also want to wish her good luck in the future with her PhD project. Finally, I would also like to thank all of my colleagues in the lab, especially Diego, Teresa, and Géraldine, for their support and willingness to help me throughout this year.

Last but not least, I would like to thank my wonderful family and friends who have constantly supported me. They were always there to listen to me, and were always ready to give me advice whenever I encountered a problem. I also want to thank them to encourage me throughout this period.

There is so much that I have learned this year that I am extremely grateful for. Not only science-related skills and insight, but I have also grown so much as a person. I am so happy that I have been able to experience all these things.

TABLE OF CONTENTS

LIST OF ABBREVIATIONS

6-OHDA	6-hydroxy-dopamine
AAVs	Adeno-associated viral vectors
CK-1	Casein kinase 1
CNP	2',3'-cyclic nucleotide 3'-phosphodiesterase
CNS	Central nervous system
DLB	Dementia with Lewy bodies
GC	Genomic copies
GCIs	Glial cytoplasmatic inclusion bodies
hαSyn	Human α-synuclein
IHC	Immunohistochemistry
ITRs	Inverted terminal repeats
KO	Knock-out
LB	Lewy bodies
LN	Lewy neurites
MAG	Myelin associated glycoprotein
MBP	Myelin basic promoter
MPP^+	1-methyl-4-phenylpyridinium ion
MPTP	1-methyl-4-phenyl-1,2,3,6-tetrahydropyridine
MSA	Multiple System Atrophy
MSA-C	MSA with cerebellar features
MSA-P	MSA with parkinsonism features
NAC	Non-Aβ component of Alzheimer's disease amyloid region
NACP	Non-Aβ component of Alzheimer's disease amyloid precursor

NCIs	Neuronal cytoplasmic inclusions
Non-inj.	Non-injected
PBS-T	PBS 0.1% TritonX-100
PD	Parkinson's disease
PFA	Paraformaldehyde
PFF	Preformed fibrils
PLD2	Phospholipase D2
PLP	Proteolipid protein
PMCA	Protein misfolding cyclic amplification
rAAV	Recombinant adeno-associated viral vector
RT	Room temperature
SN	Substantia nigra
SNpc	Substantia nigra, pars compacta
ST	Striatum
Tg	Transgenic
TH	Tyrosine hydroxylase
αSyn	α-synuclein

ABSTRACT

Current disease-mimicking rodent models for multiple system atrophy (MSA) have been shown to successfully induce a parkinsonian type of MSA (MSA-P) characteristic disease pathology, such as the presence of glial cytoplasmic inclusion bodies (GCIs) and nigrostriatal neurodegeneration by overexpression of human α-synuclein (hαSyn), driven by an oligodendrocyte-specific promoter. However there is a need for a more robust, fast and transient model to aid the development of new therapeutic strategies. Here, we hypothesized that a single striatal stereotactic injection of a recombinant adeno-associated viral vector (rAAV), designed to overexpress hαSyn through an oligodendrocyte-specific myelin-associated glycoprotein (MAG) promoter (rAAV2/9-MAG2.2-hαSyn), would be able to mimic the MSA-P-characteristic neuropathology in adult female Sprague-Dawley rats. However, we observed that the rAAV2/9-MAG2.2-GFP control vector injection in the striatum (ST) resulted in motor deficits over 6 months, and nigrostriatal dopaminergic neuronal loss in the substantia nigra (SN), indicating that this control vector induced an unexpected toxicity. To solve this problem, a viral vector dilution study was performed to assess the optimal vector titer. A new striatal stereotactic injection of a 5 or 10 times diluted titer was performed using the same vector constructs. No toxicity was observed in the GFP groups after dilution of the vector, and the 5x diluted vector appeared to induce motor deficits in the hαSyn group. Therefore, we opted to continue the generation of the novel model with this 5x diluted titer. Characterization of this 5x diluted titer model revealed no motor deficits, and no underlying nigrostriatal dopaminergic neuronal loss in both SN and ST. Interestingly, αSyn+ GCI-like structures were observed in both SN and ST, but this did not result in detectable oligodendrocyte dysfunction, as measured by the % demyelination using a Luxol Fast Blue staining. There is a need for further characterization of these GCI-like structures, and application of a more suitable quantification method for demyelination. In conclusion, these results indicate that striatal stereotactic injection of this hαSyn overexpressing viral vector construct in rats was not sufficient to induce MSA-P disease-like symptoms within the observed time frame and conditions. However, apparent GCI-like inclusions and a subtle alteration in myelin content were observed, which could be useful for understanding the underlying mechanisms of disease progression and aggregation formation. Additionally, in the future this model could be used in combination with injection of disease-affected brain homogenates, or amplified material from human source to accelerate the disease progression.

I. INTRODUCTION

For many decades, researchers have relied on animal models to study the underlying molecular pathways in both physiological and pathological states. Animal models have also been proven useful in the development of new therapeutic strategies, for instance by mimicking the disease pathology to test the effects of newly generated therapeutics.

In this thesis, the focus will lie on the rare neurodegenerative disease multiple system atrophy (MSA). First, the discovery of the α-synuclein protein in synucleinopathies will be addressed, along with its functions and morphology in a normal, physiological state. Afterwards, the transformation from this protein into a neurotoxic entity will be discussed, together with some hypotheses about disease progression in synucleinopathies. This group of three neurodegenerative disorders, including MSA, Parkinson's disease (PD), and dementia with Lewy bodies (DLB), will also be reviewed. Lastly, an extensive literature study is undertaken to obtain a more comprehensive knowledge about the existing MSA disease models in rodents, in order to be able to generate a more robust, and more efficient rodent model for MSA.

II. LITERATURE STUDY

1. Alpha-synuclein in protein aggregation disorders

1.1 Amyloid-like structures in disease biology

In humans, a broad range of diseases arises from misfolding proteins. Due to the failure of these proteins to remain in their native conformational, soluble and normal functional state, they might be converted into partially folded, precursor proteins. These conformationally changed proteins can act as templates on which more proteins will aggregate, creating protofilaments. These protofilaments can be further converted into intra- or extracellular, insoluble amyloid fibrils or aggregates. The structure of amyloid fibrils is highly organized and stable, due to backbone hydrogen bonding and hydrophobic interactions with the common protein structure (1,2), thus causing cellular instability, which might lead to cellular toxicity and degeneration.

In this thesis, the focus lies on the accumulation of the protein α-synuclein (αSyn) in the rare neurodegenerative disorder multiple system atrophy (MSA). In this disorder, αSyn is present in the form of glial cytoplasmatic inclusion bodies (GCIs) in oligodendrocytes. Other synucleinopathies, including Parkinson's disease (PD), and dementia with Lewy bodies (DLB), which are characterized by the presence of αSyn in Lewy bodies (LB) or Lewy neurites (LN), are also briefly discussed.

1.2 Discovery of synucleinopathies

More than 40 years after the discovery of spherical, proteinaceous inclusions in neurons of PD patients by Friedrich Lewy in 1912, these structures were characterized with electron microscopy by Cohen and Calkins. These inclusions, or amyloid fibrils, contain proteins that are characterized by a fibrillar ultrastructure, ranging in width between five and twelve nm. The fibrils are built up of even smaller protofibril structures (3,4), however the composition thereof remains unknown.

In 1997, αSyn was identified as one of the major components of these LB and LN (5,6), when the first rare familial cases of PD were discovered. These cases involved point mutations in the α-synuclein SNCA gene. For example, Polymeropoulos et al. identified the A53T mutation in the N-terminal region (Fig. 1), which led to a significant increase in predisposition of αSyn to polymerize into LBs (7).

These αSyn-containing LB and LN were also identified as the neuropathological hallmark of dementia with Lewy bodies (DLB). Subsequently, other filamentous aggregates, similar to LB and LN, were detected in neurons from MSA patients. These inclusion bodies were found in the nuclei and cytoplasm

of oligodendrocytes, and showed strong immunoreactivity for αSyn, linking the disease pathology of PD and DLB with MSA. This all led to the creation of the general term α-*synucleinopathies* for these three α-synuclein pathologies (8).

1.3 The synuclein family

α-Synuclein was first found in cholinergic nerve terminals by Maroteaux et al. in 1988. They isolated the protein out of the electric organ of the Torpedo (9). Shortly afterwards, mammalian αSyn could be isolated from rat brains. It was found to be highly expressed in the central nervous system (CNS), including the following regions: hippocampus, amygdala, cerebral cortex, and olfactory bulb (10). It was only known to be involved in Parkinson's disease and other synucleinopathies after the discovery of familial genetic point mutations of PD in the αSyn SNCA gene in 1997 (7).

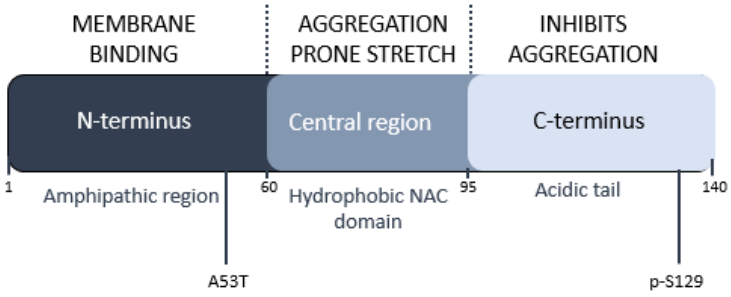

Figure 1: The human synuclein amino acid sequence.

The amino acid sequence of α-, β-, and γ-synuclein can be divided in three regions with different functions: the amphipathic N-terminal domain interacts with membranes, the hydrophobic NAC-region is an aggregation prone stretch, and the C-terminal acidic tail inhibits aggregation. A53T is a mutation found in certain familial PD cases. Phosphorylation of the Serine residue 129 (p-S129) is involved in the filament formation of α-synuclein, and can be used as a pathological marker for synucleinopathies. (Adapted from Longhena et al., Int J Mol Sci 2019)

Synuclein proteins are very abundant in the brain, however their cellular functions are not well understood. The synuclein protein family consists of α-, β-, and γ-synuclein. Their sequence length ranges from 127 to 140 amino acids, and they have 55-62% sequence resemblance. In the N-terminal region, an 11-amino-acid, imperfect consensus sequence (KTKEGV) can be found repeatedly, separated by a five to eight amino-acid long inter-repeat region (11). The C-terminal is identical in α-, and β- synuclein. These two proteins are present in nerve terminals, near synaptic vesicles, while γ-synuclein can be found throughout the whole nerve cells (11) (Fig. 1).

In the central region, a 12-amino-acid sequence (^{71}VTGVTAVAQKTV^{82}) can be found in the hydrophobic non-Aβ component of Alzheimer's disease amyloid (NAC)-region, which is presumed to be essential for the fibrilization of synucleins (12). αSyn was formerly known as NACP, or non-Aβ component of Alzheimer's disease amyloid (NAC) precursor, and is now identified as a human brain presynaptic

protein (13,14). This suggests a link between this protein and its accumulation in Alzheimer's disease affected brains. More specifically, the hydrophobic NAC domain, could have an importance in the aggregation process (12,15) (Fig. 1).

1.4 Function in cells and the CNS

It has been demonstrated that αSyn closely interacts with lipid membranes through its N-terminal KTKEGV repeats, which can be in accordance with its presumed function in the release of neurotransmitter vesicles at the presynaptic terminal (16,17). Albeliovich et al. found that the normal function of αSyn could be the negative regulation of dopamine (DA) neurotransmission (18), by modulating the synaptic release of DA vesicles. This synaptic modulation may involve phospholipase D2 (PLD2) activity. Isoforms α-, and β-synuclein might play a role in selectively inhibiting PLD2 (19). In pathological conditions, a reduction of synuclein's ability to inhibit PLD2 might be due to the reduced affinity for phospholipids after phosphorylation of synuclein (20).

Phosphorylation as a post-translational modification has been demonstrated to be present in the carboxy terminal region, which might prove that these synuclein proteins can be regulated. Okochi et al. found that this phosphorylation mostly occurred on serine residues. Using site-directed mutagenesis, they discovered two essential phosphorylation sites on Ser129 (Fig. 1) and Ser87 at the C-terminal region of α-syn. They also identified casein kinase 1 (CK-1) and CK-2 as the kinases involved in this phosphorylation process (21). *In vivo,* under physiological conditions, α-synuclein is mostly not phosphorylated, which might open the possibility that the phosphorylated Ser129 could be involved in inducing synucleinopathy. By conformationally changing αSyn, phosphorylated Ser 129 could promote filament and oligomer formation (22), possibly inducing nigrostriatal degeneration in Parkinson's disease (23).

These synuclein proteins are also expressed in other neural cells, such as oligodendrocytes (24). Human αSyn (hαSyn) might be involved in the regulation of cell adhesion by interacting with integrin family members. Thus overexpression of hαSyn in oligodendrocytes might result in cytotoxicity due to impaired cell-extracellular matrix interactions, proceeding in disrupted interactions with neighbouring neurons. This might be one of the underlying mechanisms involved in the loss of oligodendrocytes in MSA (25), which can be substantiated by the work of Asi et al., in which they suggest an upregulated SNCA mRNA expression occurs in pathological circumstances of MSA (26).

In contradiction to what is described above, Miller et al. found no SCNA mRNA expression in oligodendroglia in both control and MSA-affected human brains, implying that αSyn involvement in GCIs in MSA might be due to ectopic expression (27), or due to an αSyn transfer over a neuron-to-oligodendrocyte connection (28). However, Peng et al. indicate that internalization of αSyn monomers

in cultured oligodendrocytes might be insufficient to create GCIs (29). In conclusion, the origin of αSyn in oligodendrocytes, and the molecular mechanisms underlying the aggregation of these inclusion bodies still remains unknown.

2. Accumulation of α-synuclein

NACP, or αSyn, is natively unfolded (30), however Spillantini et al. found various morphologies of the αSyn molecules, one of which is organized in parallel β-strands (6). Hereby, a crucial question arises: How is this natively unfolded, disordered protein transformed into highly organized amyloid fibrils with a cross-β-structure (31)?

2.1 The protein folding landscape

Protein folding can be represented by a folding landscape (Fig. 2, light blue), displaying the energy levels of a protein for all its possible conformations in a funnel-like shape. The native state is a thermodynamically favourable state, however the unfolded protein must go through various intermediary states, and often pass over several kinetic barriers with the help from chaperone molecules to acquire this native conformation (32).

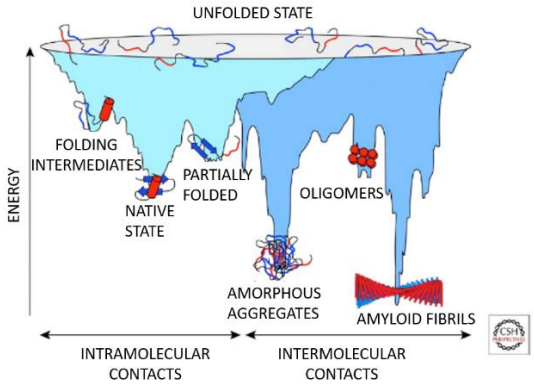

Figure 2: The protein folding landscape

The change in energy levels during protein folding (light blue) and aggregation (dark blue). Unfolded proteins will travel downhill on the energy surface towards the thermodynamically more stable native state. This process is driven by intramolecular interactions, often rendering intermediary or partially folded proteins. Chaperone molecules will promote correct folding by lowering the free-energy barriers. The protein folding process is competing with the aggregation reaction. Due to intermolecular contacts, various intermediary forms of aggregates, such as oligomers, and amorphous aggregates can be obtained, before the thermodynamically most stable amyloid fibril conformation is acquired. (From Vabulas et al., CSH Perspectives, 2010)

The aggregation energy landscape (Fig. 2, dark blue), represents the different energy levels of some intermediary conformations (oligomer, and amorphous aggregates) during the aggregation process through intermolecular interactions into amyloid fibrils. Due to many factors, such as aging, protein

aggregation, and others, some proteins may convert into the thermodynamically more stable state of amyloid aggregates, since these factors may enable them to overcome the kinetic barriers (33).

2.2 Aggregation process

During disease progression of α-synucleinopathies, the αSyn protein monomers will fold incorrectly, due to the presence of an aggregation-prone NAC region (12,15), which determines the competition between correct protein folding, and aggregation (34). This will lead to aggregation of the misfolded proteins into protofibrils or neurotoxic oligomers. When these protofibrils are clustered together through intermolecular interactions in a β-pleated sheet conformation, an amyloid fibril is generated. These amyloid fibrils will become a part of neuronal Lewy bodies and Lewy neurites for PD and DLB, and in MSA they will cluster together to form glial cytoplasmic inclusions (GCIs) in oligodendroglia (Fig. 3; (35)).

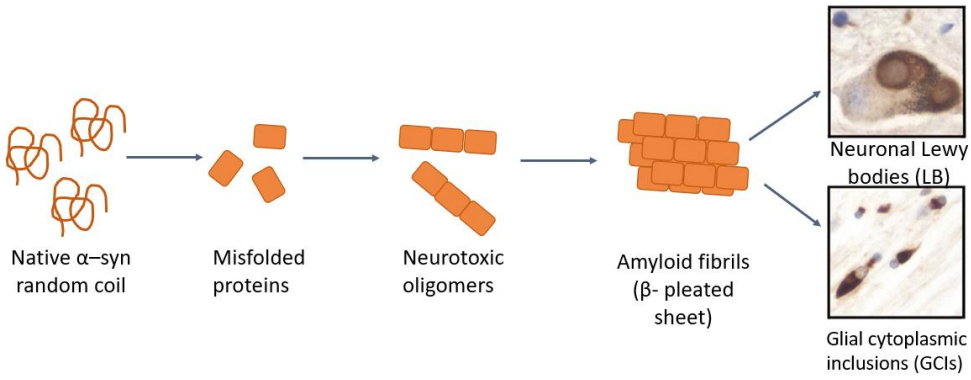

Figure 3: The α-synuclein aggregation process

Under physiological conditions, native αSyn has a random coil conformation. This native protein undergoes misfolding during α-synucleinopathy disease progression, and will be converted into higher-ordered structures with β-pleated sheet conformation (oligomers and amyloid fibrils). These structures can eventually be found in the pathological inclusion bodies. (LB for PD and DLB, GCIs for MSA). (Adapted from Giasson and Lee, Neuron, 2001)

2.3 Prion-like spreading

In case of an aggregation disorder, the amyloid fibril structure of a protein can be linked to disease progression. Two *post-mortem* studies by Kordower et al., and Li et al. revealed that fetal grafted neurons in a Parkinson's disease-affected patient display abnormal αSyn expression 14 years after transplantation. This implies that the typical PD pathological changes can develop in the grafted fetal neurons, supporting a prion-like transmission from cell to cell (36,37).

A prion is an infectious protein. The misfolded conformation of this prion protein enables it to refold native proteins into this abnormal prion configuration (38). For instance, the amyloid structure of a certain protein, such as αSyn fibrils, could act as a template on which native αSyn proteins are

misfolded. This seeding-process allows the generation of these misfolded proteins, which will proceed in spreading throughout the whole body, imposing conformational changes on the endogenous native proteins, which is often the origin of aggregation disorders (39).

This seeding-process of pathological αSyn has been observed after striatal stereotactic injection of MSA patients' brain extracts into endogenous mouse αSyn knock-out mice that overexpressed human wild-type αSyn. These mice showed accumulated inclusion bodies containing phosphorylated hαSyn, supporting the prion-like spreading hypothesis (40). This prion transmission of human pathological αSyn could only occur in mice lacking the corresponding mouse protein, when they express the human variant of the prion protein, due to species-specific factors during prion replication (41). However, this prion-like spreading mechanism as the underlying pathology of synucleinopathies is still under debate (42).

2.4 α-Synuclein strains

Prion diseases are characterized by having a variety of 'strains', or polymorphs of a protein, that have differences in structure, cellular toxicity, seeding and propagation properties. Since α-synucleinopathies have such a variety of clinical phenotypes caused by a single aggregating protein, it is hypothesized that the αSyn protein has different conformations that could account for these clinical-pathological differences (43).

Bousset et al. showed that two structurally different αSyn assemblies (fibrils and ribbons) have differences in binding, penetration, and toxicity in cells. These assemblies also have the ability to impose their conformation in a prion-like manner to endogenous αSyn proteins *in vivo*, demonstrating that the existence of such assemblies might provide a molecular basis that could account for the heterogeneous group of disorders induced by αSyn aggregation (43). Peng et al. revealed that αSyn assemblies from GCIs are about a 1,000-fold more potent in the seeding ability *in vitro*, which is expected from the highly aggressive character of MSA. In addition to that, differences in cellular environment can also promote the generation of distinct strains (29).

3. α-Synucleinopathies

α-synucleinopathies are a class of neurodegenerative disorders, including Parkinson's disease, dementia with Lewy bodies, and multiple system atrophy. These disorders mostly affect the aging population, and are pathologically characterized by proteinaceous lesions, consisting of α-synuclein-aggregated molecules, located in neurons (LBs and LNs) and glia (GCIs) (8,44).

3.1 Parkinson's disease

Parkinson's disease is the second most prevalent, age-related neurodegenerative disease, and movement disorder. PD affects about 1% of the 65-years-old population, and increases up to 4 to 5% in the 85-year olds. Worldwide, around 4.5 million people are diagnosed with PD, and since living conditions improved, the prevalence is expected to double in just 20 years (45).

3.1.1 Clinical presentation

The main clinical features of PD are related to motor deficit, and comprise resting tremor, (muscle) rigidity, impaired postural reflex or dyskinesia, and akinesia. These PD symptoms are also referred to as 'parkinsonism' features, however this term is typically used for other disorders (46).

3.1.2 Pathology

The underlying disease pathology of PD is characterized by a loss of dopaminergic neurons in the substantia nigra, pars compacta (SNpc). The SNpc region projects to the nucleus caudate and putamen of the striatum of the basal ganglia, which are necessary for gating the proper initiation of movement. In PD, a decrease of dopamine is observed in the striatum, due to the dopaminergic cell death in the nigrostriatal pathway, which provokes motor dysfunction (Fig. 4; (47)). Only when about 80 – 85% of the dopamine reserve is depleted in the striatum, which occurs after a 50 - 60% loss of dopaminergic neurons in the SNpc, the typical symptoms can be detected (46).

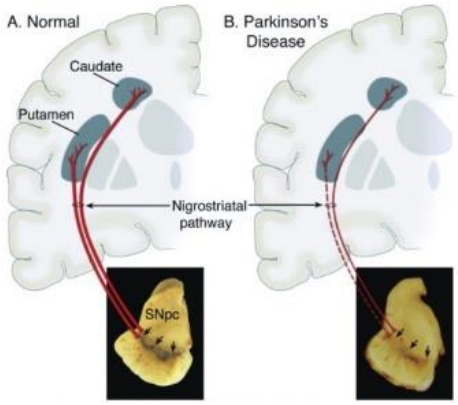

Figure 4: Underlying pathology in Parkinson's disease.

Projections from the substantia nigra, pars compacta (SNpc) to the nucleus caudate and putamen in normal (A), and pathological (B) conditions. (From: Dauer and Przedborski, Neuron, 2003)

3.1.3 Lewy bodies

This dopaminergic neuron loss observed in PD could be linked to the presence of intracellular, αSyn containing Lewy bodies and Lewy neurites (31). These eosinophilic, proteinaceous inclusion bodies were first described by Friedrich Lewy in 1912. In disease affected brains, misfolded αSyn aggregates

are converted into amyloid fibrils. Considering the potential seeding ability of those fibrils, these amyloid structures could induce conformational changes of endogenous αSyn proteins, and this results in fibril growth (39).

3.1.4 Etiology

Since the etiology and the molecular mechanisms underlying PD pathogenesis, are still largely unknown, the identification of PD-associated genes may help in understanding the disease progression (46). Although most PD cases are sporadic, and only a small percentage is caused by gene mutations, a series of point mutations and duplications/triplications have been reported. Examples of autosomal dominant gene mutations include mutations in the αSyn SCNA gene (PARK1/4), such as the A53T point mutation (7), mutations in the leucine-rich repeat kinase 2 LRRK2 (PARK8) gene (48), and VPS35, or PARK 17 (49). Additionally, some autosomal recessive gene mutations have also been identified, such as in Parkin (PARK2), PINK1 (PARK6), DJ1 (PARK7), ATP13A2 (PARK9), FBXO7 (PARK15) and PLA2G6 (PARK14), as cause of PD (49). A general overview of monogenic causes for autosomal dominant and recessive, and X-linked PD can be found in the review by Puschmann, A. (50).

3.2 Dementia with Lewy bodies

Dementia with Lewy bodies accounts for 10 - 15 % of dementia cases in elderly, making it the second most common dementia subtype, asides from Alzheimer's disease (51). Data from the Rochester Epidemiology Project by Savica et al. suggests an incidence rate of 3.5 per 100,000 people in the USA (52). The prevalence of DLB as a dementia subtype was found to be 5.4% of all types of dementia in a group of Medicare fee-for-service beneficiaries (age > 68 years) (53).

3.2.1 Clinical presentation

The two most essential characteristic symptoms of DLB are fluctuating cognitive impairments and visual hallucinations. Other features are delusions, apathy, and anxiety (51). The dementia symptoms precede the motor dysfunctions and the parkinsonism in DLB, which is the opposite of what occurs in PD (54).

3.2.2 Pathology

The underlying disease pathology is the abundant presence of LBs and LNs in the cerebral cortex (31). These inclusions are similar to those found in PD, however, the disposition of these aggregates differs in DLB affected brains.

3.3 Multiple system atrophy

Multiple system atrophy is a sporadic, adult-onset, rare, and rapidly progressing neurodegenerative disease that affects both men and women, and it is clinically characterized by a combination of parkinsonian features, cerebellar signs, and autonomic failure (55–57). The estimated prevalence varies over multiple studies, ranging between 1.9 to 4.4 cases per 100,000 people (58,59).

MSA was introduced as a term in 1969 as a term by Graham and Oppenheimer to depict various similar neurodegenerative disorders as one disease. These disorders include nigrostriatal degeneration, olivopontocerebellar atrophy, and Shy-Drager syndrome (60). The reason for this combination into one disorder was the acknowledgement of the presence of GCIs in oligodendrocytes as the pathological hallmark regardless of the differences in clinical features.

3.3.1 Clinical presentation

In MSA, two variants of motor deficits can be distinguished: MSA with parkinsonism features (MSA-P), and MSA with cerebellar, autonomic, urinary, and pyramidal dysfunction (MSA-C) (57). The prevalence of each subtype varies geographically. MSA-C is more prevalent in the Asian population, while the MSA-P subtype predominantly occurs in European and Northern American populations (61).

MSA-P is characterised by symptoms closely related to the nigrostriatal degeneration of PD, including tremor, bradykinesia with rigidity, speech impairment, and postural instability, due to loss of reflexes. Despite the similarities to PD, no or little therapeutic response is observed to levodopa therapy (57,62,63).

The cerebellar dysfunction in the MSA-C subtype is characterized by ataxia of gait, limb movements, and speech. Orthostatic hypotension is a highly common sign of autonomic failure, asides from impotence in men, and urinary incontinence in women. Another phenotype of MSA patients is pyramidal dysfunction (57).

3.3.2 Pathology: Glial Cytoplasmic Inclusions

The presence of glial cytoplasmic inclusions in oligodendroglias of patients with characteristics of MSA was first described by Papp et al. in 1989 (64). GCIs show a strong immunoreaction with anti-α-synuclein antibodies, indicating that these inclusions are mainly composed of αSyn accumulations. In addition to GCIs, neuronal cytoplasmic inclusions (NCIs) are sporadically found in the substantia nigra, dentate fascia, and the pontine and inferior olivary nuclei. NCIs also strongly react to these αSyn antibodies (65). A reduction in solubility of αSyn may induce a conformational change to form filaments, and cause aggregation (66), which might be the common underlying pathogenic component

of neurodegeneration, resulting in a rapid progression of motor-, autonomic, and non-motor-deficits as described above. Tubular structures are found in the GCI inclusions at the ultrastructural level (64), which could be altered microtubular tangles, consisting of filaments covered by granular material (67). GCIs are composed of αSyn and other proteins, including ubiquitin, hypophosphorylated tau, 14-3-3 proteins, and multiple other components (68).

For the parkinsonian MSA-P subtype, another underlying disease pathological feature is the loss of dopaminergic neurons in the nigrostriatal pathway, resulting in the decreased connection of the SNpc with the nucleus caudate and putamen of the striatum, which is essential for gating the initiation of muscle movements (69). Since oligodendrocytes are affected by the presence of GCIs in MSA, they might be the origin of oligodendroglial dysfunction. Considering these cells are responsible for myelin sheath formation in nearby neurons (70), this dysfunction might provoke axonal deterioration, resulting in dopaminergic neuronal death.

3.3.3 Etiology

Although most MSA cases are sporadic, a few families with probable MSA have been reported (71–73). In one family, mutations in COQ2 has been identified as a very rare variant associated with an increased risk of developing MSA (74). However, for other cases, the underlying genetic component remains to be elucidated. This implies that the disease genes could only be inherited in rare instances, or this opens the possibility that MSA has a multigenic etiology (71). No polymorphisms were found in the SNCA gene coding sequence in MSA patients (75), indicating that these mutations are unlikely to contribute to the disease progression. This implies that other elements, such as environmental factors or neurotoxins could be involved in the induction of mitochondrial dysfunction, leading up to oxidative stress (76).

4. Rodent models for MSA

Researchers have relied on animal models to study the biological, and molecular pathways of diseases for many decades. Additionally, these animal models have been proven useful in the development of new therapeutic strategies. Whenever a new genetic mutation has been identified to be associated with a certain disease, animal models can be generated e.g. using viral vectors, as a substitute to *in vitro* research, or modelling with cell lines. In the case of MSA, no genetic background has been identified. These rodent models need to reproduce the neuropathological hallmarks of MSA, which is nigrostriatal degeneration for MSA-P and motor deficits (77), and the presence of oligodendroglial inclusion bodies (GCIs) (64).

4.1 Toxin-based rodent models

One of the earliest methods of generating nigrostriatal lesions has been the use of neurotoxins. *In vivo* phenotypic MSA-P models have been developed by sequential or simultaneous application of neurotoxins to induce degeneration of the substantia nigra and/or the striatum (77).

6-hydroxy-dopamine (6-OHDA) is a dopaminergic neurotoxin that selectively induces oxidative stress in dopaminergic neurons. Since it does not cross the blood-brain-barrier, it is directly applied unilaterally via intracerebral injection in the SN to create a *hemiparkinsonian* model. 6-OHDA induces acute degeneration of the striatal projections to the ST, leading up to loss of dopaminergic cell bodies. A rotational behaviour towards the ipsilateral side of the unilateral lesion is induced by amphetamine treatment, which displays the asymmetry in movements due to loss of nigrostriatal projections (78). A more chronic model can be acquired when injecting 6-OHDA in the ST, inducing retrograde cell death over several weeks (79).

Wenning et al. created a double toxin-double lesion rat model of MSA-P, by inducing nigrostriatal degeneration via unilateral injection of 6-OHDA in the median forebrain bundle, followed by an injection of quinolinic acid into the ST at the ipsilateral side (80). This model resembles early MSA-P pathology (81).

A single toxin-double lesion model is generated by a single, unilateral injection of neurotoxin 1-methyl-4-phenylpyridinium ion (MPP^+) into the ST, which induces both nigral and striatal degeneration (82), resulting in motor behaviour similar to what is observed in the double toxin-double lesion model (83). The 1-methyl-4-phenyl-1,2,3,6-tetrahydropyridine (MPTP) systemic model already existed for PD, in which the lipophilic MPTP crosses the blood-brain-barrier, where it is converted into MPP^+ by monoamine oxidase B (84). After conversion, the MPP^+ selectively accumulates in dopaminergic neurons (85), where it inhibits the mitochondrial function, and thus generates oxidative stress, affecting the nigrostriatal pathway bilaterally.

These toxin-based models replicate the loss of nigrostriatal projections and dopamine depletion, however the main shortcoming is that they do not encompass the characteristic GCI-like pathology of MSA. However, these toxin-induced models have improved our understanding of the interaction between nigral and striatal neurons. Additionally these models have proven useful in testing novel therapies that target MSA-like neuronal degeneration (77).

4.2 Disease-affected brain homogenates

Becker et al. discovered that a prion-like seeding activity of αSyn is present in MSA patient's brains. This implicates that αSyn inclusions, and its amyloid fibrils, could act as a template upon which

endogenous αSyn proteins can misfold, and as such it induces aggregation and spreading of the pathological GCIs. This seeding activity can be used to create a novel disease model, e.g. by stereotactically inoculating rodent brains with homogenates of human MSA-affected brains. This is presumed to induce fibril growth in a prion-like manner, by promoting conformational changes in the endogenous αSyn proteins (39,86). For instance, Watts et al. were successful in transmitting MSA prions to transgene mice, since widespread phosphorylated αSyn deposits could be found throughout the brain after inoculation with MSA brain homogenates (87).

This model could be useful in determining the effects of the surrounding cellular (co)factors in the MSA-affected brains on disease progression, asides from the misfolded αSyn proteins, since whole brain homogenates are used. On the other hand, no specific effects of these misfolded proteins can be determined, rendering a more general characterization of all affected brain components.

4.3 PMCA and preformed fibrils

The technique of protein misfolding cyclic amplification (PMCA) is used to amplify a specific molecular weight fraction of a sample to create assemblies of a specific strain of misfolded α-syn. For MSA disease modelling, MSA-affected human brain homogenates can be used for PMCA to produce high yields of the specific αSyn strain that is present in these brain samples (86).

Alternatively, recombinant monomers of αSyn can be used to generate aggregated preformed fibrils (PFFs). First, shorter fibrils can be generated through sonication of the PFFs, since these short fibrils will trigger endogenous phosphorylation of αSyn at S129 (88). Hereby, the conversion of endogenous hαSyn into pathogenic forms of αSyn is accelerated (89,90) after striatal stereotactic injection of these fibrils in hαSyn transgenic rats.

These techniques allow the characterization of patient-specific strains, and detection of strain-to-strain differences. Another advantage of these models is the inducibility, implying that prophylactic treatment strategies can be examined.

4.4 Transgenic rodent models

Palmiter and Brinster were the first ones to report a transgenic (tg) mouse line, in which they successfully introduced the growth hormone gene (91). Transgenic animals can be used to knock-out, or knock-in a specific gene to study the role of proteins. Additionally, these models could be used to mimic familial, inherited disorders to study the underlying disease mechanisms, which can be useful in the search for novel therapeutic strategies based on these inheritable pathological characteristics.

Although most MSA cases are sporadic, a few families with probable MSA have been reported (71–73), from which genetically modified transgenic rodent models could be developed. In addition to that, it has been hypothesized that pathological (over)expression of αSyn in oligodendrocytes will lead to GCI production. In 2002, Kahle et al. were the first to describe the generation of a tg mouse model of MSA, in which WT αSyn was specifically overexpressed in oligodendrocytes under a proteolipid protein (PLP) promoter. They reported the presence of pathological phosphorylated αSyn, confirming this hypothesis (92). These results convinced other research groups to generate tg mice expressing (human) αSyn, under different oligodendrocyte-specific promoters, such as the 2',3'-cyclic nucleotide 3'-phosphodiesterase (CNP) promoter (93), or the murine myelin basic promoter (MBP) (94). In short, αSyn accumulation caused by these tg promoters resembles the key neuropathological characteristics of MSA. This includes abnormal aggregation in the most-affected areas in MSA, accompanied by myelin loss, neurodegeneration, and motor deficits (94). However, this overexpression of hαSyn is not observed in MSA patients (27). Another drawback is the constitutive expression throughout the whole life of the animal, considering the late-onset character of MSA.

4.5 Viral vector-based models

Lastly, viral vector-based methods exist to specifically transduce target cells, using a target-specific promoter, at an exact time point, e.g. by a Cre-LoxP inducible promoter. Adeno-associated viral vectors (AAVs) have been used on a large scale as the preferred gene delivery platform. AAV is a non-integrating, non-enveloped, defective parovirus, encapsulating a single-stranded linear DNA genome in an icosahedral capsid. AAV is a dependovirus, since it remains in a proviral, inactive state after infection, unless coinfection occurs with an adenovirus, or another helper virus, then the AAV genome will be expressed (95,96).

Recombinant AAVs (rAAVs) could be generated using a vector plasmid, containing the gene-of-interest, flanked by two inverted terminal repeats (ITRs) *in cis*, by providing the viral *trans* elements, including *rep, cap,* and the helper virus (97). rAAVs are convenient to use for MSA disease modeling, because they provide safe, and long-term expression of transgenes in the CNS (98). Limitations of rAAVs include pre-existing immunity for several human AAV serotypes (99), a limitation in insert size (4.1 to 4.9 kb) (100), and a possibility of having a broad tropism. In order to avoid these limitations, the vector constructs can be improved. For instance, new serotypes can be generated by capsid shuffling. By changing the viral capsid proteins, the specificity of interaction with host cells is shifted (101).

Viral-based models can be used to evaluate the function of proteins in the cells, or evaluate therapeutics for the treatment of CNS disorders, by overexpressing or knocking down disease-related genes by loco-regional gene transfer in rodents.

4.5.1 MBP promoter

MSA is characterized by pathological, αSyn-positive GCIs in oligodendrocytes (64–66). This led to the generation of viral vectors designed to express human αSyn under the control of oligodendrocyte specific promoters, such as the murine myelin basic promoter (MBP) (102). Hereby, these vectors will specifically target oligodendrocytes in mice (103). This MBP promoter was used by Shults et al. in the generation of a transgenic mouse model, rendering the key functional and neuropathological, neurodegenerative characteristics of MSA (94).

The effects of these rAAVs, driving hαSyn expression via the MBP promoter in oligodendroglia, include a widespread synucleinopathy, and accumulation of insoluble and phosphorylated hαSyn, leading up to a progressive nigrostriatal degeneration (103).

4.5.2 MAG promoter

In the CNS, oligodendrocyte recognition, formation of myelin as spiralling loops, and maintenance of myelin, is mediated by myelin-associated glycoprotein (MAG) (104). These characteristics of this pre-myelinating marker were the motivation to investigate the possibility of using the MAG promoter for oligodendrocyte-specific AAV-mediated transgene expression (105).

The MAG promoter originates from humans, is small in size, and has oligodendroglial selectivity (105), which makes it an excellent choice to induce and mimic the MSA α-synucleinopathy, or other oligodendroglial-specific diseases in rodents. The small size makes the viral vector very mobile. Asides from that, this viral vector method is thought to be a fast and robust way of inducing genes-of-interest in the promoter-targeted cells. Another advantage includes the transient characteristic of the non-integrating viral vectors, making them time-dependent and inducible.

III. RESEARCH QUESTION

In this study, we aimed to develop a more efficient, faster and more robust viral vector-based rodent model for the neurodegenerative disorder multiple system atrophy, using viral vector technology. This novel model will be useful in the development of new therapeutic strategies, and increasing the knowledge of the underlying disease pathology.

The generation of the model is achieved by striatal stereotactic injection of recombinant adeno-associated viral (rAAV) vectors expressing human αSyn specifically in oligodendrocytes through the use of an oligodendroglial-specific promoter. Hereby, the neuropathological hallmark of MSA is anticipated to be reproduced by inducing α-synuclein accumulation in oligodendrocytes, promoting the formation of glial cytoplasmic inclusion bodies (GCIs). These GCIs are expected to provoke oligodendroglial pathology and demyelination, eventually leading to nigrostriatal degeneration, which is the underlying characteristic of the parkinsonian MSA-P subtype.

This model will be characterized over a period of 5 to 6 months post-injection. Behavioural motor deficits will be measured using a cylinder test, and an adhesive-removal test. Neuropathological characterization will include GCI-formation by means of αSyn-immunostaining, measurement of dopaminergic neuron loss through tyrosine hydroxylase (TH) immunostaining and demyelination using a Luxol Fast Blue staining. In addition during these experiments, the optimal vector titer dilution will be assessed to use in future experimental set-ups.

IV. EXPERIMENTAL WORK

1. Materials and methods

1.1 rAAV Stereotactic injections

1.1.1 Animals

All animal experiments were approved by the Bioethical committee of the KU Leuven (Belgium). Adult, female Sprague-Dawley rats (n_{total} = 48 animals) were housed two per cage in a temperature-controlled room under a 12-hour light/dark cycle with free access to food and water.

1.1.2 rAAV viral vectors

Two recombinant adeno-associated viral vector (rAAV) constructs, containing an AAV2/9 serotype, encoding either the human α-synuclein (hαSyn), or a green fluorescent protein (GFP) transgene under the control of the 2.2 kb myelin associated glycoprotein (MAG) promoter were produced at the Leuven Viral Vector Core from the KU Leuven (Leuven, Belgium) as previously described (106).

1.1.3 Stereotactic injections

All surgical procedures were performed using aseptic techniques. A mixture of ketamine (60 mg kg^{-1}, Ketalar, Pfizer, Puurs, Belgium) and medetomidine (0.4 mg kg^{-1}, Dormitor, Pfizer, Belgium) was used for anaesthesia. Following anaesthesia, the hair at the incision area was removed, and a 2 % xylocaine local anaesthetic gel was applied. The rats were then placed in a stereotactic head frame (Stoelting, Wood Dale, IL, USA), the incision was made, and cleaned with 1 % iodine alcohol. For the stereotactic viral vector injection, a small hole was drilled in the right hemisphere. The location of this burr hole was determined using the following stereotactic coordinates, calculated with bregma as a reference point: +0.07 anteroposterior, -0.28 lateral, and -0.52 dorsoventral. 4 µl of viral vector (undiluted: 3 x 10^{12} genomic copies (GC) / ml; 5x diluted: 6 x 10^{11} GC / ml; 10 x diluted: 3 x 10^{11} GC / ml) was injected intrastriatally with a 10-µl Hamilton syringe with an injection rate of 0.25 µl min^{-1}. The rAAV2/9-MAG2.2-hαSyn construct was used for stereotactic injection of rats in the hαSyn-group, and rAAV2/9-MAG2.2-GFP construct for the GFP-group. These constructs will from now on be referred to as vectors from the hαSyn-, and GFP-group. The needle was left in place for an additional 5 min before being retracted. The incision wound was closed with stitches, and the anaesthesia reversed using 5 mg kg^{-1} Antisedan (Orion Pharma) in saline per 100 g of body weight. The rats were placed on a 37 °C hot plate to maintain body temperature until they were awake. They were closely monitored until 24 h after the surgical procedure.

1.2 Behaviour assessment

1.2.1 Adhesive removal test

The adhesive removal test was used to assess the effects of viral vector injection on the sensorimotor performance. A small circular piece of adhesive tape was applied to the snout of the rat, and the time-of-removal was measured (107). The average of 3 measurements is calculated to assess motor deficits.

1.2.2 Cylinder test

The cylinder test was used to measure asymmetry in spontaneous forelimb use at 2 weeks, and every months following stereotactic injection, until sacrifice at 5 or 6 months post-injection. The contacts by fully extended digits of each forepaw with the wall of a 20 cm-wide clear glass cylinder were first videotaped, and afterwards scored by an observer that is blind to the different groups, as described by Schallert et al. (108). 30 wall touches were counted per animal. The number of impaired forelimb contacts, ipsilateral to the lesion, was expressed as a percentage of total forelimb contacts. Non-lesioned control rats should score an average of 50% in this cylinder test. No habituation of the animals to the glass cylinder was allowed before video recording.

1.3 Histopathological analysis and immunofluorescent labeling

The rats were euthanized with an intraperitoneally injected overdose of pentobarbital (60 mg kg^{-1}, Nembutal, CEVA Santé, Belgium), and transcardially perfused with saline solution, followed by 4 % paraformaldehyde (PFA; Sigma-Aldrich) in PBS. The brains were extracted, postfixed overnight in 4 % PFA, stored in a 0.1 % Na-azide solution until sectioning. 50 µm thick coronal brain sections were made with a vibrating microtome (HM 650V, Microm, Germany) for histopathological analysis.

1.3.1 αSyn and GFP immunohistochemical staining

To assess the transduction volume of the viral vectors, striatal and nigral free-floating sections were first treated with 3% hydrogen peroxidase for 10 min at room temperature (RT) to quench endogenous peroxidase activity, then rinsed once and washed twice with PBS 0.1% Triton X-100 (PBS-T; Acros Organics). Nonspecific binding was blocked for 1 h with PBS-T and 10 % normal goat serum (DakoCytomation, Belgium). The sections were incubated overnight at RT in primary antibody solution with 10% normal goat serum. The primary antibodies for the sections from the hαSyn-, and GFP-group were raised against human α-synuclein (mouse polyclonal, 1:2000, SYN 211, Millipore), and against GFP (rabbit polyclonal, 1:2000, in house) respectively.

As secondary antibody, we used biotinylated goat anti-mouse or anti-rabbit IgGs (1:1000, DakoCytomation). After 30 min incubation at RT, the sections were rinsed once, and washed twice

with PBS 0.1 % TritonX-100. This was followed by incubation with streptavidin-horseradish peroxidase complex (1:1000, DakoCytomation) in 1x PBS 0.1 % Triton X-100 (30 min, RT). The sections were mounted on glass slides coated with gelatin, and dehydrated in 70 % ethanol, 90 % ethanol, two times in 100% ethanol, and finally in xylene (Histo-Clear II, National Diagnostics) for 5 min each step. The coverslips are mounted with DPX mounting medium (DPX Mountant for histology, Sigma-Aldrich), and left to dry overnight.

1.3.2 TH staining

To assess the dopaminergic neuron loss in the substantia nigra, free-floating sections were stained as described above using a tyrosine hydroxylase (TH) antibody (mouse polyclonal, 1:2000, Abcam). An antigen retrieval step was executed, in which the sections were incubated for 30 min in a 10 mM citrate buffer (pH = 6.0) at 80 °C, followed by 20 min on ice. This was followed by a 3 % hydrogen peroxidase quench step (10 min). The blocking solution contained 1:20 swine serum (Dako), and PBS-T. Overnight incubation with the TH primary antibody, is followed by incubation with the secondary swine anti-mouse antibody (1:500, Dako) for 30 min at RT. To visualize TH immunoreactivity, Vector SG hydrogen peroxidase substrate kit (SK-4700, Vector Laboratories) was used for 4 min, followed by a rinse and two wash steps with PBS to stop the revealing reaction. The sections were mounted on glass slides, dehydrated, and the coverslips were mounted with DPX mounting medium, as described above.

1.3.3 Luxol Fast Blue staining

To analyse the myelin integrity and assess demyelination in the striatum, striatal sections of both hαSyn-, and GFP-groups were mounted on gelatin-coated glass slides, and allowed to dry. The slides were rinsed with 95 % alcohol, and placed in a 0.1 % Luxol Fast Blue solution in acidified methanol (Luxol Fast Blue Stain Kit; Atom Scientific) for 2 hours at 60 °C. The slides were rinsed in 70 % denatured ethanol (Atom Scientific) for 3 sec, and washed with tap water. The sections were differentiated using 0.05 % lithium carbonate solution (Atom Scientific) for 10 min, and washed with tap water (109). The slides were dehydrated in 70 % ethanol, 90 % ethanol, two times in 100% ethanol, and finally in Histo-Clear II for 5 min each step. The coverslips are mounted with DPX mounting medium, and left to dry overnight.

1.4 Stereological quantification

1.4.1 Nigral TH count

To assess the dopaminergic neuronal cell loss in the SN, the number of TH-immunopositive cells was estimated using optical fractionator, which is a random sampling stereological counting method in a computerized system (StereoInvestigator; MicroBright-Field, Magdeburg, Germany). Images were

acquired using the LEICA DMR Microscope (Leica, Wetzlar, Germany). Both injected and non-injected sides were quantified in every 5th section (total = 7 sections), incorporating the whole substantia nigra over the rostro-caudal axis for quantification. The conditions of the experiment were blinded to the investigator.

1.4.2 Striatal TH count

Seven sections covering the whole striatum were immunostained against TH as previously described. Images were acquired using the LEICA DM4 B optical microscope (Leica, Wetzlar, Germany) with a Leica DFC320 digital camera (Leica) and the Leica Application Suite software (Leica). In order to cover the striatum completely, tile images were captured using a Leitz 5x objective (Leica). Analysis was performed using the software ImageJ. Prior conversion to 8-bit, the images were transformed to black and white using the Threshold option. Setting a threshold allows the visualization of the selected grey level values within the region of interest between 0, which represents pure white, and 255 pure black, respectively. After that a region of interest (ROI) was determined enclosing the striatum. With this setup, we were able to measure the intensity in each hemisphere.

1.4.3 Striatal demyelination quantification

Sections covering the whole striatum were stained with the Luxol Fast Blue staining kit as previously described. Images were acquired using the LEICA DM4 B optical microscope (Leica, Wetzlar, Germany) with a Leica DFC320 digital camera (Leica) and the Leica Application Suite software (Leica). In order to cover the striatum completely, tile images were captured using a Leitz 5x objective (Leica). Analysis was performed using the software ImageJ, identical to what is described in the Striatal TH count section.

1.5 Statistical analysis

Normality of the data was checked using a Shapiro-Wilk test. Outliers were removed using a Grubb's test. The data are expressed as the means ± standard error of mean. The between-group comparisons of the motor performances over multiple timepoints, and the number of TH+ cells in the injected vs. non-injected site were made through 2-way ANOVA analysis. To compare multiple factors, a Bonferroni correction was used. A nonparametric t-test was used to analyse differences of % TH+ cell loss, and the % demyelination between the two groups. The statistical analyses were performed using the GraphPad Prism® software, and a p-value < 0.05 was considered statistically significant.

2. Results

2.1 Overexpression of α-synuclein in oligodendrocytes in vivo with a viral vector

2.1.1 Striatal injection of rAAV2/9-MAG2.2-hαSyn results in widespread transduction

For the generation of a novel viral vector based model of the parkinsonian MSA-P subtype, we used a rAAV2/9-MAG2.2-hαSyn viral vector construct (Fig. 5B). Herein, a human αSyn SNCA gene is under the control of an oligodendroglial-specific myelin-associated glycoprotein (MAG) promoter (105). Adult, female Sprague Dawley rats (n = 10 animals / group) received a single 4 µl stereotactic injection of rAAV2/9-MAG2.2-hαSyn, or rAAV2/9-MAG2.2-GFP (3 x 10^{12} GC / ml) in the striatum (Fig. 5A-B). To assess the effectiveness of these vectors, the transduction volume of the vectors throughout the striatum was visualized 6 months after injection through a histological αSyn or GFP immunofluorescence staining. This revealed a widespread transduction of the transgene throughout the injected hemisphere in serial sections as shown in Figure 5C by intense αSyn+ fluorescence, in comparison to the non-injected (non-inj.) hemisphere, which showed no specific fluorescent signal.

2.1.2 Effects of oligodendroglial hαSyn expression on motor and sensorimotor performances

To assess the motor response to a sensory stimulus, an adhesive removal test was performed every 2 months during 6 months after viral vector injection (Fig. 6A). This revealed no significant differences in time-of-removal between the hαSyn- and GFP-groups.

To further assess motor deficit, the spontaneous forelimb use is measured using a cylinder test (Fig. 6B). Somewhat unexpectedly, overall significant motor deficits could be observed in the GFP expressing control group in comparison to the hαSyn group (2-way ANOVA, *$p < 0.05$).

2.1.3 Assessment of dopaminergic neurodegeneration when overexpressing hαSyn in oligodendroglia

Using the Optical Fractionator tool in StereoInvestigator, we assessed the stereological counts of tyrosine hydroxylase (TH) immunopositive neurons (Fig. 7B) via a systematic randomly sampled set of counting frames. TH is an endogenous enzyme used to catalyse the conversion of tyrosine into L-DOPA in the catecholamine biosynthesis of dopamine (Fig. 7A), making it a well-suited marker to visualize dopaminergic cells in the nigrostriatal pathway. Stereological counts of TH+ dopaminergic neurons in the SN, indicated that striatal injection of the GFP control vector induced an unanticipated significant loss of TH+ dopaminergic neurons in the nigrostriatal pathway (2-way ANOVA, *$p < 0.05$; Fig. 7B).

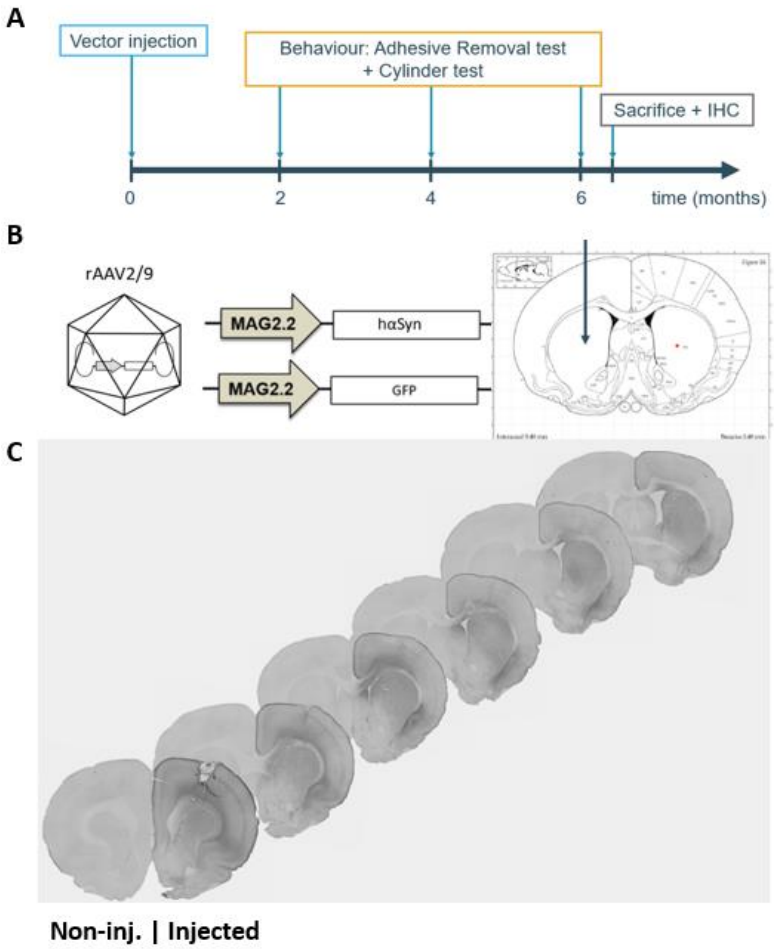

Figure 5 Striatal injection of rAAV2/9-MAG2.2-hαSyn results in widespread transduction.

(A) Experimental set-up: stereotactic injection of rAAV2/9-MAG2.2-hαSyn in the striatum of rats in the hαSyn group, and rAAV2/9-MAG2.2-GFP in the control group (n = 10 animals / group). This is followed by a characterization of the motor deficits over 6 months, using behavioural assessments, such as the adhesive removal test, and the cylinder test. Lastly, the rats were sacrificed to perform immunohistochemical (IHC) analyses. **(B)** Recombinant adeno-associated viral vector (rAAV) construct, containing a MAG2.2 promoter that drives either hαSyn or GFP expression specifically in oligodendrocytes, after stereotactic injection into the striatum of rats. **(C)** αSyn expression throughout serial sections of the ST 6 months post-injection in the hαSyn expressing rat brain, in the injected vs. non-injected (non-inj.) hemispheres. MAG = myelin-associated glycoprotein; hαSyn = human α-synuclein; GFP = green fluorescent protein.

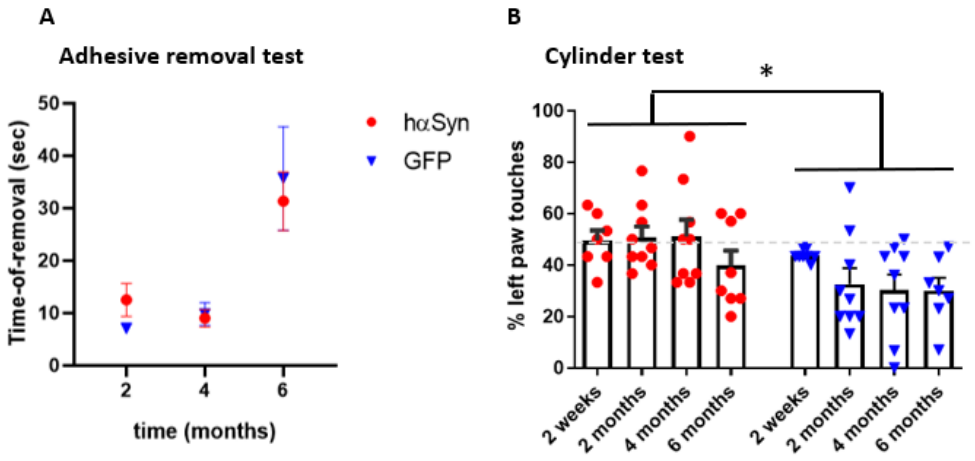

(Figure 6, legend on next page)

Figure 6 Effects of hαSyn overexpression in oligodendroglia on motor performance.

Assessment of motor performance over 6 months using an adhesive removal test **(A)** and a cylinder test **(B)**, with the adhesive removal test **(A)** demonstrating no significant differences in sensorimotor impairment between the hαSyn (red) and GFP (blue) groups. **(B)** The cylinder test displays significant motor impairments in the rAAV2/9-MAG2.2-GFP injected rats, compared to the hαSyn group (2-way ANOVA, *p < 0.05) vs. baseline performance measured at 2 weeks.

Post-hoc analysis revealed a nonsignificant difference in % TH+ cell loss in the SN of rAAV2/9-MAG2.2-GFP injected control rats (Fig. 7C). The % TH+ cell loss compares the number of TH+ cells in the injected to the non-injected side in each group. Interestingly, no significant differences are detected in TH+ cell counts and % TH+ cell loss between the injected and the non-injected sides of the hαSyn group (Fig. 7B-C).

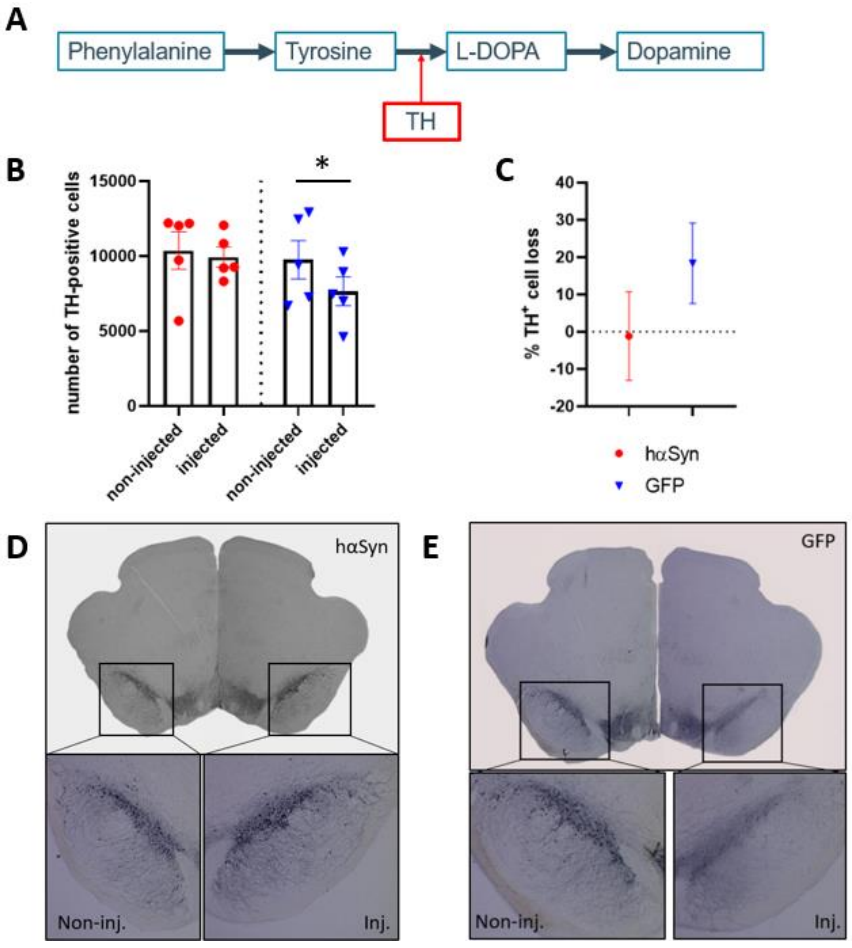

Figure 7 Effect of oligodendroglial hαSyn expression on neurons in the substantia nigra

(A) Biosynthesis of dopamine. A scheme demonstrating the conversion of Tyrosine into L-DOPA, catalysed by the tyrosine hydroxylase (TH) enzyme. **(B)** Stereological counts of TH+ cells in the SN, indicate a significant loss of total TH+ cells in the GFP group. **(C)** % TH+ cell loss (inj. vs. non-inj.) in the SN of hαSyn (red) and GFP rats (blue). **(D-E)** Microscopic images of TH immunostaining in the SN of hαSyn **(D)** and GFP **(E)** rats reveal a decrease in intensity in the GFP group. The boxes represent a tile of 5x magnification of the SN. Non-inj. = non-injected side; Inj. = injected side (2-way ANOVA, *p < 0.05)

Microscopic images of TH-immunopositive cells in the SN reveal an overall decreased intensity of staining in the GFP control group on the injected side as compared to the hαSyn group (Fig. 7D-E), in

accordance to what has been observed in the TH+ cell count (Fig. 7B). Together with the behavioural results (Fig. 6B), this opens up the possibility that the viral vector of the GFP control group might induce toxicity.

2.2 Vector dilution optimization study

A combination of factors might have contributed to the neuronal cell loss observed in the SN of the GFP control group. We hypothesized that the observed neurotoxicity could be attributed to viral overload in the injected side. In order to solve this problem, we opted to perform a vector dilution optimization study, using two dilutions of the vector titer over a period of 1 month to optimize the viral vector titer to use for the stereotactic injections.

The experimental set-up remains similar to the previous experiment (Fig. 8A). Adult, female Sprague Dawley rats (n = 4 animals / group) received a single 4 µl stereotactic injection of rAAV2/9-MAG2.2-hαSyn or rAAV2/9-MAG2.2-GFP (6 x 10^{11} or 3 x 10^{11} GC / ml; 5x and 10x dilution, respectively) in the striatum. Motor deficits were assessed every 2 weeks using a cylinder test, and immunohistochemical analyses were performed post-sacrifice.

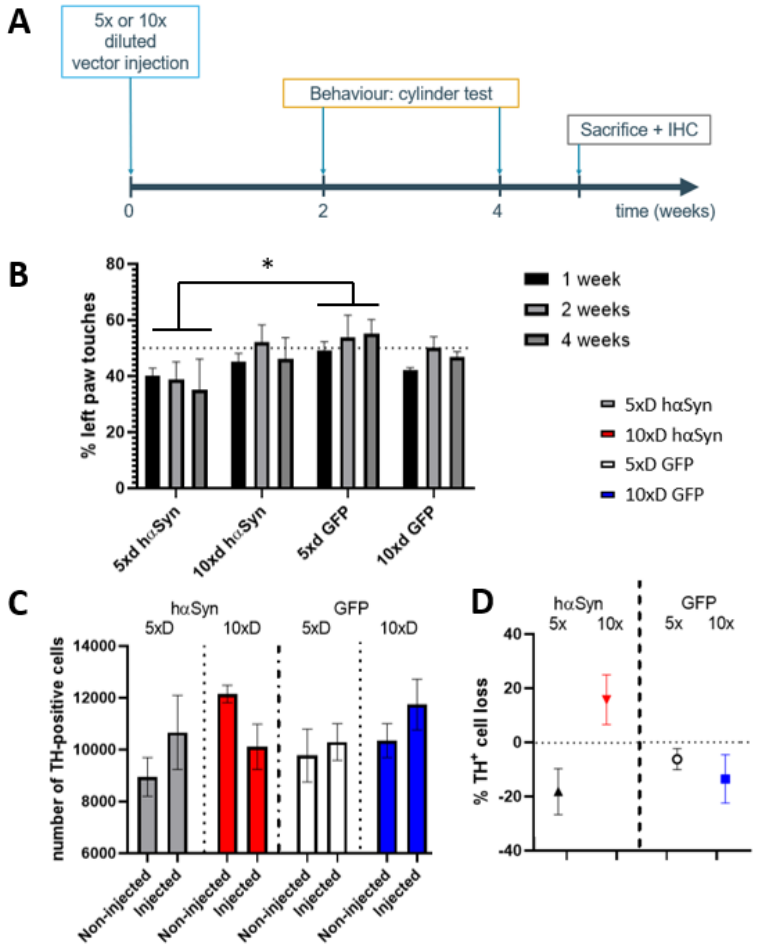

(Figure 8, legend on next page)

Figure 8 Viral vector titer optimization study

(A) Experimental set-up: stereotactic injection of a 5x and 10x diluted vector titer of rAAV2/9-MAG2.2-hαSyn in the striatum of rats in the hαSyn group, and rAAV2/9-MAG2.2-GFP in the GFP control group (n = 4 animals / group), followed by characterization of the motor deficits over 1 month, using a cylinder test. Lastly, the rats are sacrificed to perform IHC analyses. **(B)** The cylinder test reveals a significant motor impairment in the 5x diluted hαSyn group compared to the 5x diluted GFP group. **(C)** Stereological counts of TH+ cells and **(D)** % TH+ cell loss in SN of hαSyn and GFP rats 1 month post-injection reveal no significant differences (2-way ANOVA, *p<0.05).

2.2.1 Effects of different diluted viral vector titers on motor performances

To assess the motor deficit induced by the 5 or 10 times diluted viral vector, a cylinder test was used to measure the spontaneous forelimb use over 1 month (Fig. 8B). No significant differences are observed in the GFP control group in both dilutions, solving the toxicity problem encountered before. Additionally, a significant motor impairment was observed in the 5x diluted hαSyn group when compared to the 5x diluted GFP group (2-way ANOVA, *p < 0.05).

2.2.2 Assessment of dopaminergic neurodegeneration induced by different viral vector titers

Stereological counts of TH+ dopaminergic neurons in the SN, revealed no significant differences in the total number TH+ cell in the different dilutions of both groups (Fig. 8C). A trend of % TH+ cell loss is observed in the 10x diluted hαSyn group, and the number of cells remains stable in the GFP control group (Fig. 8D), however the variability is high due to the low number of animals used in this experiment. With the results from the cylinder test in mind, and aiming for the highest, non-toxic dose that is still able to induce pathology, we have chosen to continue with the 5x diluted vector titer.

2.3 New 5x diluted viral vector model

To generate the new viral vector-induced MSA disease model after optimization of the vector titer, adult, female Sprague Dawley rats (n = 10 animals / group) received a single 4 µl stereotactic injection of rAAV2/9-MAG2.2-hαSyn or rAAV2/9-MAG2.2-GFP (6 x 10^{11} GC / ml) in the striatum. Motor deficits were assessed every month for 5 months using a cylinder test. After 5 months, the rats were perfused with paraformaldehyde to perform immunohistochemical analyses (Fig. 9A).

2.3.1 Striatal injection of 5x diluted viral vectors results in widespread transduction

To assess the transduction effectiveness of these vectors, the volume of transduction was visualized 5 months post-injection through a histological αSyn or GFP immunofluorescence staining. This revealed a widespread expression of the transgene throughout the injected hemisphere in serial sections of the SN and ST, visualized by an intense fluorescence signal (Fig. 9C-D).

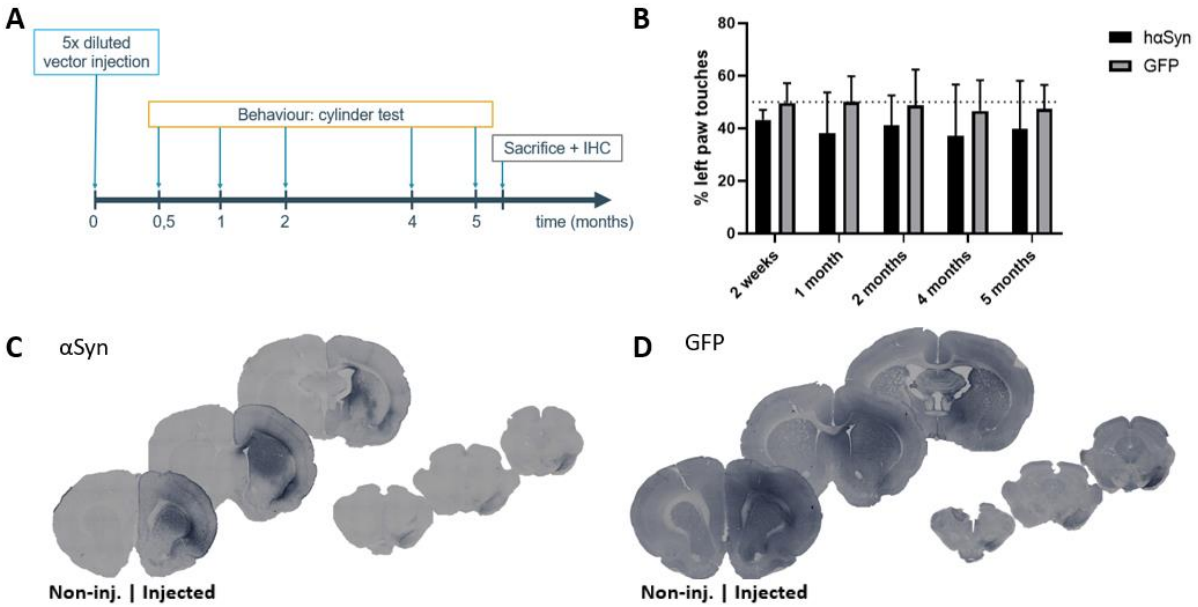

Figure 9 Effects of striatal injection of 5x diluted viral vector

(A) Experimental set-up: stereotactic injection of a 5x diluted vector titer of rAAV2/9-MAG2.2-hαSyn in the ST of rats in the hαSyn group, and rAAV2/9-MAG2.2-GFP in the GFP control group (n = 10 animals / group), followed by characterization of the motor deficits over 5 months, using a cylinder test. Lastly, the rats are sacrificed to perform IHC analyses. **(B)** The cylinder test reveals no significant motor impairment in the 5x diluted hαSyn group compared to the 5x diluted GFP group. **(C-D)** Immunofluorescence staining of αSyn and GFP in the ST (left) and SN (right) reveals widespread transduction in the injected hemisphere. (2-way ANOVA)

2.3.2 Effects of the 5x diluted vector injection on motor behaviour

Measurement of the spontaneous forelimb use with a cylinder test revealed a tendency of motor deficit in the hαSyn expressing group, while no significant motor deficits can be observed in the GFP group, which suggests a viral vector-based induction of motor impairment in this hαSyn group (Fig. 9B). This might be caused by the viral vector-induced accumulation of hαSyn in the oligodendroglia, resulting in a cellular dysfunction. This could provoke a low extent of secondary neuronal degeneration of dopaminergic neurons, important for motor control, in the nigrostriatal pathway.

2.3.3 Assessment of nigral and striatal dopaminergic neurodegeneration in the 5x diluted vector model

Stereological counts of TH+ dopaminergic neurons in the SN of the viral vector-injected animals revealed no significant differences in the total number of TH-immunopositive cells in the SN between the injected and non-injected sides of both hαSyn and GFP groups (Fig. 10A-B). Post-hoc analysis revealed a nonsignificant difference in % TH+ cells between the hαSyn and GFP group in the SN (Fig. 10C).

Additionally, the TH+ expression in the ST was assessed in both groups, by comparison of the TH-staining intensity in each hemisphere (Fig. 10D-E), using ImageJ software. This revealed no significant differences in % TH+ cell loss between the hαSyn and GFP groups in the ST (Fig. 10F).

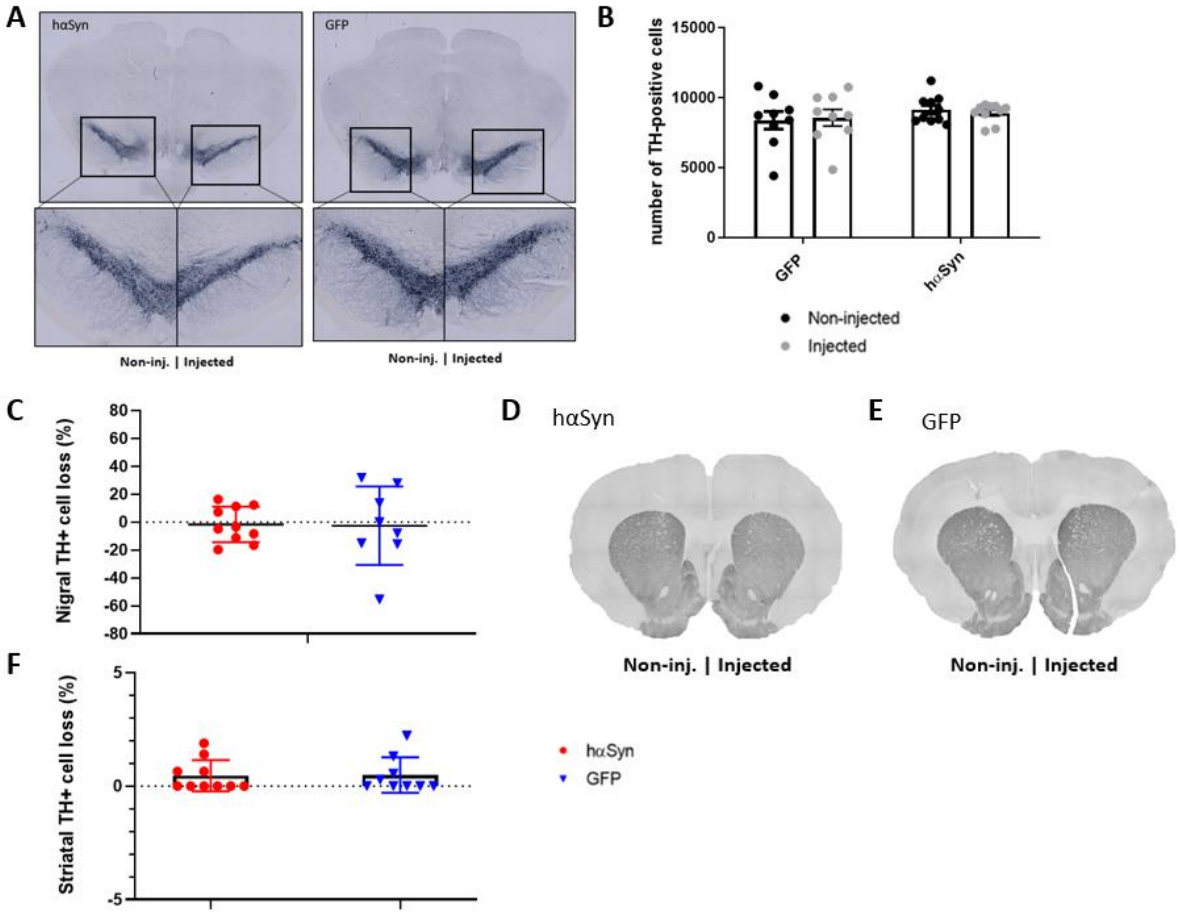

Figure 10 Effects of hαSyn overexpression on dopaminergic neurons in the SN and ST

(A) Microscopic images of TH immunostaining in the SN of hαSyn and GFP rats reveal similar intensity. The boxes represent a tile of 5x magnification of the SN. **(B)** Stereological counts of TH + cells in the SN, and **(C)** % TH+ cell loss in the SN reveal no significant differences. **(D-E)** Representative microscopic image of TH immunostaining of the ST of both hαSyn and GFP groups. **(F)** % TH+ cell loss in the ST, based on the intensity of immunostaining, is not significantly different. Non-inj. = non-injected side; Inj. = injected side.

2.3.4 αSyn staining in striatum and substantia nigra reveals the presence of GCI-like inclusions

αSyn immunostaining followed by microscopic analysis of the SN and ST from rAAV2/9-MAG2.2-hαSyn-injected rats, revealed the presence of dense αSyn+ globular structures (Fig. 11). These αSyn-containing structures are hypothesized to be GCI-like inclusion bodies, which is the histopathological hallmark of MSA (64). Striatal oligodendrocyte dense patches, striosomes, do not display these αSyn+ globular structures (Fig. 11B). Further histopathological analysis is required to confirm the GCI-like nature of the αSyn-containing inclusions.

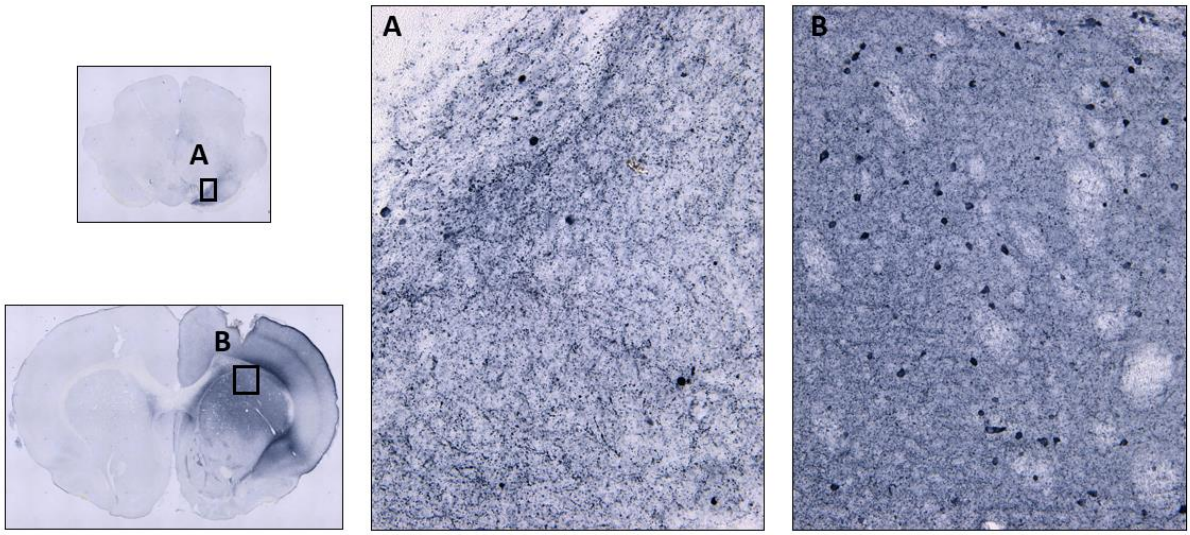

Figure 11 αSyn-containing oligodendrocytes in the SN and ST

Reconstructed mosaic tile microscopic image of the SN (upper panel) and the ST (lower panel). Higher magnification (20x) of microscopic images of the SN **(A)** and ST **(B)** reveals the presence of dense αSyn-containing inclusions. Striatal striosomes (white patches) do not display αSyn+ inclusions.

2.3.5 Assessment of oligodendroglial dysfunction

Since we observed what might be GCI-like structures in the SN and ST of hαSyn rats in the previous experiment (Fig. 11), and GCIs are known to elicit oligodendroglial dysfunction, we aimed to examine the effects of hαSyn overexpression on the cellular function of oligodendroglia. Since oligodendroglia are responsible for myelination, and maintenance of myelin sheets in the CNS (70), we performed a Luxol Fast Blue staining to quantify (de)myelination.

Microscopic images were acquired to visualize the Luxol Fast Blue myelin staining in the striatal region (Fig. 12A). Overall mild differences in intensity, and size and number of striosomes could be observed by eye in the Luxol Fast Blue staining images. Using the ImageJ software, the intensity of the staining was assessed in both groups and compared between the injected and non-injected hemispheres. However, an unpaired t-test revealed no significant differences in intensity (Fig. 12B), indicating that the myelin content remained unchanged in both groups in the ST.

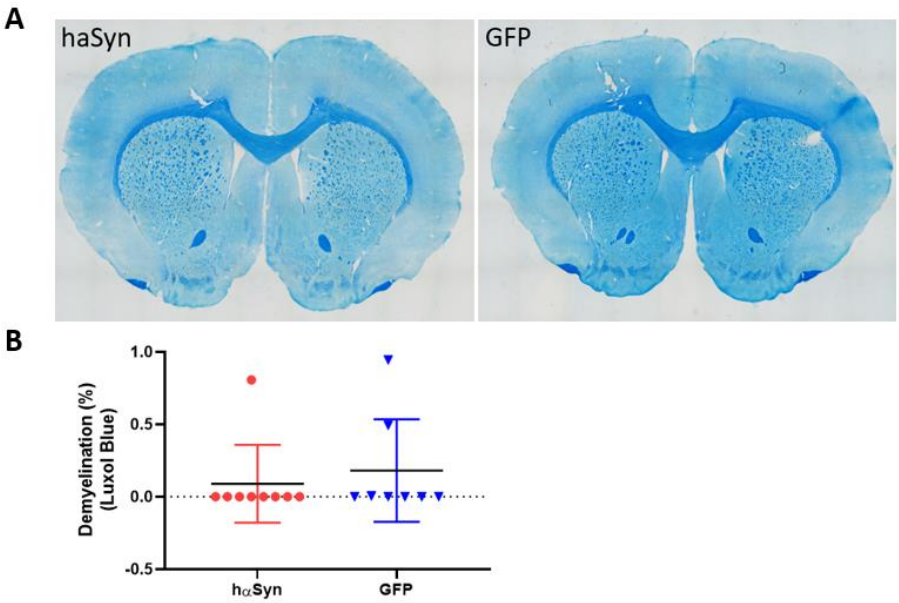

Figure 12 Myelin staining of the striatum

(A) Microscopic images of the ST after Luxol Fast Blue staining of myelin. **(B)** Quantification of the % demyelination in the ST revealed no significant degeneration of myelin in both groups. (unpaired t-test)

V. DISCUSSION

Currently, a wide spectrum of protein misfolding disorders exists, in which proteins are converted into insoluble amyloid fibrils or aggregates, causing cellular toxicity (1). One group of protein misfolding disorders is the α-synucleinopathy family, which contains adult-onset neurodegenerative disorders, such as Parkinson's disease, dementia with Lewy bodies, and multiple system atrophy. These disorders are characterized by the presence of aggregated α-synuclein (8).

In this thesis, we focussed on MSA, which is a rare, and rapidly progressing neurodegenerative disease, characterized by the presence of α-synuclein containing glial cytoplasmic inclusion bodies (GCIs) in oligodendrocytes (64,65). In the disease pathogenesis, this α-synuclein protein undergoes conformational changes, by which they gain a pathological feature, hereby undermining the physiological function of these oligodendroglia.

Although many clinical aspects of MSA have been described, an effective treatment has not yet been established in exploratory clinical studies. The development of therapies has been hindered by various factors, including the incomplete knowledge of the pathophysiological underlying mechanisms that cause GCI formation. Other factors comprise the absence of early stage, presymptomatic diagnostic tests, and the shortage of animal models that mimic the human pathology (110).

Currently, a few animal models exist for the MSA-P subtype, however there is a need for a more robust, fast and transient model to aid the development of new therapeutic strategies. The earliest MSA disease models consisted of toxin-based rodent models in which nigrostriatal degeneration was reproduced by the use of neurotoxins, such as 6-OHDA, quinolinic acid, and MPTP (78,80,82). Although these toxin-based models have proven useful in reproducing MSA-like neuronal degeneration and provided insight in the nigrostriatal interactions, they do not encompass the generation of GCIs, which is an essential pathological hallmark. Other models could exist that exploit the prion-like seeding and spreading activity of αSyn to induce widespread aggregation of misfolded αSyn in the CNS. These models can be based on stereotactic injection of disease-affected (human) brain homogenates (87). Alternatively, synthetic preformed fibrils (PFFs), or PMCA amplified misfolded assemblies with differences in conformations (strains) could be stereotactically injected to possibly induce hαSyn aggregation in a GCI-like manner, when the human αSyn protein is expressed in the animal model. The use of human patient material would allow the investigation of the differences in conformation between the different patients. Transgenic rodent models have been developed for MSA in which hαSyn is constitutively expressed under an oligodendrocyte specific promoter, such as PLP (92), CNP (93), or MBP (94). It has been hypothesized that this overexpression of hαSyn can be seen in

pathological circumstances (26) and is likely to induce GCI formation, however Miller et al. report that this overexpression has not been observed in MSA patients (27). A drawback might be the constitutive overexpression of the transgene, considering that MSA is an age-related disorder.

All of the above described models are characterized by a permanent induction of the disease pathological characteristics. Alternatively, viral vector-based models were generated in which a transgene could be transiently expressed in the preferred cell type with a cell type specific promoter at a specific timepoint. For instance, to mimic MSA disease pathology, non-integrating viral vectors that specifically transduce oligodendrocytes with an oligodendrocyte specific promoter, such as MBP (107) have been used. Since this MBP promoter is from murine origin, we have explored an alternative, smaller, oligodendroglia-specific, human myelin-associated glycoprotein (MAG) promoter (105) to induce transient overexpression of hαSyn.

1. Generation of the novel MSA disease model in rats

In this study, we attempted to generate a novel rodent model for multiple system atrophy, based on acute overexpression of hαSyn in adult rat brain, with the aim to generate a more efficient and robust model than the earlier reported methods and models. This new model was generated by striatal stereotactic injection of recombinant adeno-associated viral (rAAV) vectors expressing human αSyn specifically in oligodendrocytes through the myelin-associated glycoprotein (MAG) promoter. We hypothesized that by overexpressing hαSyn in oligodendrocytes, accumulation of these hαSyn proteins into glial cytoplasmic inclusion bodies (GCIs) will be achieved, thus rendering the histopathological features of MSA. We hypothesized that these GCIs would be able to induce oligodendroglial dysfunction, resulting in dopaminergic neurodegeneration, and its correlated motor deficits as is observed in the MSA-P subtype.

1.1 MAG model, undiluted titer

Our first attempt of generating this novel viral-based MSA disease model has proven unsuccessful. The striatal stereotactic injection of the rAAV2/9-MAG2.2-hαSyn that was designed to specifically overexpresses human α-synuclein in oligodendrocytes did not result in a significant motor deficit, as was measured by an adhesive-removal test and a cylinder test over a time-span of 6 months (Fig. 6). This implies that the rAAV2/9-MAG2.2-hαSyn viral vector was unable to induce the behavioural symptoms of MSA in rats, despite of the widespread transduction of the viral vector that has been observed (Fig. 5C).

Even though the cylinder test is presumed to be a specific test to measure long-term progressive asymmetric motor deficit (108), no motor deficits were observed in the hαSyn group throughout the 6 months after viral vector injection. A reduction of the % left paw use was expected in this hαSyn group, since the viral vectors were injected in the contralateral, right hemisphere, and induced expression of hαSyn in these oligodendrocytes. This lack of observed motor deficits might be explained by the possible secondary character of neurodegeneration in MSA (93), as the oligodendrocytes are not directly involved in the control of motor function. The initiating mechanisms that result in nigrostriatal neurodegeneration in MSA-P still remain to be elucidated, however two hypotheses exist about the pathogenesis of MSA. First, the disease can be regarded as a primary gliopathy, in which oligodendrocyte dysfunction is induced by elevated hαSyn levels, and subsequently this dysfunction is thought to trigger myelin sheath impairment, causing axonal decay, resulting in dopaminergic neuronal degeneration via the oligo-myelin-axon-neuron interaction (111). The second hypothesis poses that MSA might be a primary neuronal disease, in which pathologic αSyn is from neuronal origin, since it is a predominantly neuronal protein. Then, via a prion-like, cell-to-cell spreading mechanism, these misfolded proteins will be deposited in oligodendrocytes, resulting in GCI formation (112).

An unexpected motor deficit was observed in the GFP control group when compared to the hαSyn group, contrary to the random behaviour that is expected from these control rats. A significant decrease of spontaneous left paw use was observed in this GFP group, indicating that this viral vector batch induced progressive motor deficit (Fig. 6B). Since these unforeseen motor deficits were observed, we wanted to investigate whether the overexpression of the transgenes in oligodendrocytes had led to secondary dopaminergic neurodegeneration. The extent of dopaminergic neuronal loss was measured by stereologically counting tyrosine hydroxylase (TH)-immunopositive cells in the SN using StereoInvestigator. Indeed, a suspected, significant loss of TH+ cells was observed between the injected and non-injected side in SN in the GFP control group. On the contrary, the hαSyn group did not show significant differences in TH+ cell count between the injected and non-injected sides (Fig. 7B). The decrease in total TH+ cells is a marker of dopaminergic neuronal loss in the nigrostriatal pathway of the GFP control rats, indicating that the GFP control vector has induced neurotoxicity. We hypothesized that this toxicity could be addressed to either a too high viral titer, or an impurity of the used viral vectors batch.

1.2 Vector dilution study

To elucidate whether these effects in the GFP control group were provoked by an overload of viral vector at the injection site, a vector dilution study was performed over a shorter time-span of 1 month, in which two dilutions (5x and 10x) of the vectors were used for the striatal stereotactic injection.

No significant differences were observed in the cylinder test in the 2 diluted GFP control groups (Fig. 8B), indicating that the toxicity problem might be solved in terms of the motor deficit that was observed in the GFP group when using the undiluted titer. Additionally, a significant motor deficit was observed between the 5x diluted hαSyn group and the 5x diluted GFP group (Fig. 8B), indicating that this titer was able to induce asymmetric motor symptoms. Stereological counts of TH+ cells revealed a stable number of TH+ cells in the GFP groups of both dilutions. However, no significant loss of TH+ cells could be detected in the hαSyn group (Fig. 8C). A possible explanation for the high variability in outcome of the experiments might be the low number of animals (n = 4 animals / group). Nevertheless, taking all this data together, we opted to continue with the highest viral vector titer that did not induce toxicity in the control groups, which is the 5x dilution.

1.3 5x diluted MAG model

The generation of the novel rat model, using the optimized viral vector titer (5x diluted), resulted again in a widespread transduction of the transgene throughout the SN and ST of the injected hemisphere in both groups (Fig. 9C-D). A non-significant trend of motor deficit was observed in the hαSyn group (Fig. 9B). To further investigate the possible underlying dopaminergic neurotoxicity, a TH immunostaining was performed to elucidate the effect of the viral vector injection on the number of TH+ cells. However, stereological counts of TH+ cells in the SN revealed no significant differences between the injected and non-injected sides in both hαSyn and GFP control groups (Fig. 10A-C). Additionally, the loss of TH terminals staining intensity was also assessed in the ST using ImageJ. This once more revealed no significant differences between the two groups (Fig. 10D-F).

Further characterization of other histopathological MSA features is undertaken. The histopathological hallmark of MSA is the presence of GCIs in oligodendrocytes. To investigate whether αSyn-containing inclusion bodies could be detected, we immunostained for αSyn. Microscopic analysis revealed the presence of a low number of dense αSyn+ globular structures in the SN and ST (Fig. 11), which might correspond to GCIs, since GCIs are known to strongly immunoreact with anti-αSyn antibodies (64,65). Higher magnification of these images revealed that these αSyn+ inclusions were mostly found in oligodendrocyte-shaped cells, however some aggregates were also observed in neurons. These results are corresponding to the 95 % target specificity of transgene expression by the 2.2 kb MAG promoter, as reported by von Jonquieres et al. (105), and corresponds to the target specificity that has been assessed previously in our lab for this construct. Additionally, Ozawa et al. reported that the density of GCIs was relatively low in SN, compared to the severe neuronal loss that can be observed in disease-affected brains (113), which corresponds to the low number of αSyn+ accumulation we observed. This low density of inclusions opens the possibility that other factors also contribute to the neurodegenerative process in this region. However, an absence of nigrostriatal degeneration was

observed in the TH+ cell count in both SN and ST (Fig. 10B-C, F), which could indicate that the formation of GCIs can occur before neurodegeneration has taken place.

Additionally, the oligodendrocyte-dense striosome patches do not display the αSyn+ globular structures (Fig. 11B). Sato et al. report that the striosome region is more likely to be spared in MSA-P patients (114), which is in line with what we observed in these microscopic images. In addition to that, these striosomes were thought to be involved in providing the striatal input to the dopaminergic neurons in the SN pars compacta (115), however a deleted glycoprotein-rabies tracing study revealed that these projections predominantly origin from the matrix compartment of the ST (116), which indicates that these striosomes might not be involved in the disease progression of MSA-P.

Overall, the underlying molecular mechanisms involved in GCI formation are not elucidated yet. Some hypothesize that αSyn mRNA expression is upregulated in pathological circumstances, such as during GCI formation in MSA (26). However, others report contradictory data, suggesting that SCNA mRNA expression is absent in both physiological and pathological situations (27), indicating that the origin of αSyn could be ectopic. A possible explanation for this ectopic αSyn source might be a neuron-to-oligodendrocyte prion-like transfer mechanism, which is correlated to an earlier posed hypothesis that MSA might be a primary neuronal disease. Taking all this together, an increased intracellular level of hαSyn is thought to promote the disease progression in both cases. Correspondingly, the viral vector-based overexpression of hαSyn in oligodendrocytes in this study is thought to promote the development of hαSyn-rich accumulations. Other pathways that have been suggested to play a role in MSA pathogenesis include upregulated autophagy (117), disturbed myelin trophic support (118) and proteasome dysfunction (119). Additionally, induction of myelin dysfunction by altering the regulation of myelin lipids could promote myelin degeneration, ultimately resulting in axonal damage and neuronal loss (120).

Lastly, since oligodendrocytes are responsible for the myelin sheath formation and maintenance thereof in nearby neurons in physiological circumstances (70), and oligodendrocyte dysfunction is provoked by the presence of GCIs in MSA, we also checked for the change in myelination patterns in the ST using a Luxol Fast Blue staining. Although overall differences in intensity, and size and number of striosomes could be observed by eye in the Luxol Fast Blue staining images (Fig. 12A), no significant differences were detected when quantifying the % demyelination in both groups (Fig. 12B). However, this small alteration in myelin content (Fig. 12A) might not be detected by the quantification method we used in this experiment, indicating that we possibly need an alternative quantification method that is more accurate or sensitive in determining the possible oligodendrocyte dysfunction.

2. Options for further and/or future research

Based on the literature study, the MAG promoter seemed very promising to use to specifically target the oligodendrocytes for the generation of this novel MSA disease model, in which the oligodendrocytes are one of the most affected cell types. The overexpression of hαSyn specifically in oligodendrocytes had already proven successful in earlier rodent models, which is in correspondence with our research question.

Here, we demonstrate that targeted overexpression of hαSyn using the MAG promoter did not induce overt neurodegeneration in the SN and ST, and thus progressive motor impairments were not observed. However, the vector has been transduced throughout the whole injected hemisphere, and the accumulation of αSyn has been detected in both nigral and striatal regions, indicating that the viral vector expression has been able to induce one of the histopathological characteristics of MSA, which is the presence of GCI-like structures. The absence of neurodegeneration might be explained by differences between the MAG promoter and earlier described promoters in targeting the oligodendrocytes.

One of the possibilities of why this hαSyn overexpression model did not induce neurodegeneration, could be a time-dependent effect of disease induction. Since only few αSyn+ aggregates were observed, this could be related to the insufficiency of GCI-like aggregate formation. This implies that oligodendroglial dysfunction has not been sufficient, and thus no demyelination occurred and accordingly, no neuronal degeneration could have taken place.

Another possibility could be that the hαSyn vector titer was too low, making the vector less potent in exerting its effects, and perhaps unable to induce oligodendroglial dysfunction. This could possibly be explained by the rather high variability that has been observed in quantifying the vector titer prior to the stereotactic injection. Nonetheless, a significant effect on motor behaviour was observed in the vector dilution study in the hαSyn group. However, since the number of animals was low, and the variability was rather high, we cannot make accurate conclusions from these results.

There is a need for further analysis to provide evidence that these dense αSyn+ globular structures are indeed GCIs. For example a proteinase K digestion can be performed, to determine whether the dense αSyn+ globular structures observed in the oligodendrocytes are soluble, non-aggregated structures, or insoluble aggregates, considering that CGIs have been correlated with the insoluble aggregate structure (121). Furthermore, an additional experiment in which phosphorylation of αSyn is investigated would also add value to the research, since this phosphorylation is known to occur in the pathological conformation of αSyn. Lastly, a more suitable quantification method to measure

demyelination in the ST needs to be developed, since an alteration of myelin content could be observed by eye (Fig. 12A), however no differences were measured using ImageJ (Fig. 12B).

In future experiments, perhaps the use of other oligodendrocyte targeting promoters, for example targeting the myelin/oligodendrocyte glycoprotein (MOG) gene (70) could be of use to induce the expected neurodegeneration and accumulation of αSyn into GCIs. Another possibility to increase the probability of disease induction could be the combination of multiple factors to induce pathology and spreading of the aggregates. Perhaps the combination of this viral vector-based model with one of the earlier described models could be useful. For instance, the injection of recombinant αSyn preformed fibrils, or the injection of human disease-affected brain homogenates, together with the viral vector-based overexpression of hαSyn specifically in the oligodendrocytes. Hereby, a prion-like spreading might be induced by the disease-affected hαSyn assemblies, and the oligodendrocyte dysfunction will be enhanced by viral vector-based overexpression of hαSyn in the oligodendrocytes. An alternative strategy might include the combination of this viral vector-based overexpression of hαSyn, together with the nigrostriatal lesions, induced by neurotoxins, such as MPTP, quinolinic acid, and 6-OHDA. Perhaps other factors might also be implicated in the disease progression, which could be of use in inducing MSA in rodents.

Lastly, a less invasive method of inducing the disease pathology might also be considered, such as systemically injecting rAAVs. However, rAAVs with the 2/9 serotype do not efficiently cross the blood-brain-barrier. A newly described AAV vector serotype, AAV-PHP.B, could be implemented, that has been reported to cross the blood-brain-barrier efficiently (122).

3. Conclusion

The generation of a viral vector-based rat model for MSA-P was delayed due to an unexpected toxicity that was observed in the GFP control group. Therefore a viral vector dilution study was performed to assess the optimal vector titer to induce disease pathology. The 5x diluted vectors induced motor deficits in the hαSyn group, and the toxicity problem was solved in the GFP control group with this dilution. Since this was the highest titer that did not induce toxicity, we opted to continue with this dilution to generate a novel rat model using the same viral constructs. However, no significant motor deficits were induced, and no dopaminergic neuronal loss is observed in both SN and ST. However the presence of GCI-like αSyn+ structures was observed in both SN and ST. Further analysis is needed to characterize these structures, such as an insolubility assay or the use of phosphorylation markers. Lastly, no loss of oligodendrocyte function was measured, albeit slight differences in intensity, and number and size of striosomes could be distinguished by eye, indicating the need for a more efficient

quantification method. In conclusion, these results indicate that the overexpression of hαSyn in oligodendrocytes in rat striatum using a rAAV2/9 viral vector construct containing the MAG promoter is not sufficient to induce MSA-P disease pathology within the investigated time frame and conditions.

NEDERLANDSTALIGE SAMENVATTING

1. Introductie

Gedurende vele decennia hebben onderzoekers vertrouwd op diermodellen om de onderliggende moleculaire *pathways* in zowel fysiologische als pathologische toestanden te bestuderen. Deze diermodellen zijn ook nuttig gebleken bij de ontwikkeling van nieuwe therapeutische strategieën, bijvoorbeeld door de pathologie van een bepaalde ziekte na te bootsen.

In deze thesis ligt de focus op de zeldzame neurodegeneratieve ziekte multipele systeem atrofie (MSA), meer bepaald het parkinsonisme subtype (MSA-P), dat gekarakteriseerd wordt door de accumulatie van het proteïne α-synucleïne (αSyn) in gliale cytoplasmatische inclusielichamen (GCI) in oligodendrocyten (64). Hierdoor zal de myeline aanmaak in nabijgelegen neuronen aangetast worden (70), wat uiteindelijk nigrostriatale dopaminerge neurodegeneratie veroorzaakt, waardoor de initiatie van beweging ondermijnd wordt (69).

Naast MSA bestaan nog twee andere α-synucleïnopathieën, namelijk de ziekte van Parkinson en Lewy body dementie, waarvan de algemene histopathologische eigenschap de aanwezigheid van Lewy lichaampjes en Lewy neurieten in neuronen is (31). Het α-synucleïne proteïne bestaat uit een 140 aminozuurresidu's lange sequentie (11), waarvan de centrale niet-Aβ component van de ziekte van Alzheimer (NAC) regio essentieel blijkt te zijn voor de aggregatie van het eiwit (12). In het geval van deze aggregatieziekten, zullen foutief gevouwen protofibrillen samenklonteren en dankzij intermoleculaire interacties een β-gevouwen sheet conformatie vormen. Deze wordt uiteindelijk getransformeerd tot een toxische amyloïde structuur, die teruggevonden kan worden in de eerder beschreven inclusie lichaampjes (66).

Voor α-synucleïnopathieën wordt een prion-achtige uitzaaiing en transmissie verondersteld, waarbij het foutief gevouwen proteïne de goed gevouwen endogene proteïnen kan omvormen tot de foutieve conformatie, en dit kan zich uitspreiden doorheen het hele lichaam (38). Deze foutieve conformaties *('strains')* kunnen structureel verschillen tussen deze verschillende aandoeningen, alsook variëren in toxiciteit, en uitzaaiingseigenschappen (43).

Om de ontwikkeling van therapieën voor deze zeldzame aandoening te ondersteunen, trachten wij een robuuster en efficiënter rattenmodel te ontwikkelen, op een induceerbare wijze. Eerder beschreven knaagdierenmodellen omvatten de neurotoxine-geïnduceerde modellen, die met behulp van intracerebrale injectie met 6-OHDA, chinolinezuur, of MPTP vooral de parkinsonisme karakteristieken nabootst van MSA-P, zoals nigrostriatale neurodegeneratie (77–85). Voorts bestaan ook nog andere modellen die gebaseerd zijn op de prion-achtige transmissie van αSyn, zoals modellen

geïnduceerd via injectie met MSA-geaffecteerde hersenen homogenaat (87), of specifieke fracties van dit homogenaat dat geamplificeerd werd via PMCA (86), of synthetisch aangemaakte conformaties (PFF) (88). Een alternatief hiervoor is een transgeen dierenmodel, waarbij het SNCA αSyn gen constitutief tot overexpressie gebracht wordt specifiek in oligodendrocyten met de hulp van een oligodendrocyt-specifieke promoter, zoals de PLP, CNP, en MBP promoters, om op deze manier de neuropathologie na te bootsen (92–94). Als laatste bestaan er ook virale vector-geïnduceerde dierenmodellen voor MSA, waarbij recombinante adeno-geassocieerde virale vectoren (rAAV) op een exact tijdstip in de ontwikkeling specifieke cellen kunnen transduceren en bijvoorbeeld met de hulp van oligodendrocyt-specifieke promoters zoals MBP de MSA neuropathologie induceren (102,103).

Een nieuw voorgestelde oligodendrocyt-specifieke promoter in deze studie is de myeline-geassocieerde glycoproteïne (MAG) promoter. Met de hulp van een rAAV construct, zal humaan αSyn tot overexpressie gebracht worden in oligodendrocyten. Vervolgens zal dit nieuwe model gekarakteriseerd worden op basis van metingen van motorische defecten en histopathologische kenmerken zoals dopaminerge neurodegeneratie, aanwezigheid van GCIs en demyelinatie.

2. Materiaal en methoden

Allereerst werden striatale stereotactische injecties verricht met de virale vectorconstructen rAAV2/9-MAG2.2-hαSyn en rAAV2/9-MAG2.2-GFP, respectievelijk voor de hαSyn en GFP controle groep, in vrouwelijke Sprague-Dawley ratten. Over de volgende 5 tot 6 maanden werden twee soorten gedragsmetingen uitgevoerd (pleister verwijderingstest en cilinder test), om de verschillen in motorische tekorten te kunnen bepalen. Vervolgens werden de ratten geperfuseerd met paraformaldehyde, om histopathologische analyses uit te voeren op hersensecties (50 µm). Immunohistochemische kleuringen van αSyn en GFP werden uitgevoerd met anti-αSyn en anti-GFP antilichamen. Voorts werd er ook een tyrosine hydroxylase (TH) kleuring uitgevoerd met TH antilichamen om het aantal dopaminerge neuronen te bepalen in de SN, gebruik makende van StereoInvestigator software. De intensiteit van TH kleuring werd ook bepaald in het ST, via ImageJ software. Als laatste werd een Luxol Fast Blue kleuring uitgevoerd om het % demyelinatie te meten in het ST, met behulp van intensiteitsmeting in ImageJ.

3. Resultaten

3.1 *In vivo* overexpressie van α-synucleïne in oligodendrocyten met een virale vector

De opbouw van het model gebeurde met een enkele stereotactische injectie van 4 µl rAAV2/9-MAG2.2-hαSyn, of rAAV2/9-MAG2.2-GFP (3 x 10^{12} GC / ml) in het striatum van vrouwelijke Sprague-Dawley ratten (n = 10 dieren / groep). 6 maanden na deze injectie werd de transductie efficiëntie bepaald door middel van αSyn en GFP immunofluorescentie kleuring. Microscopische beelden tonen

een intens αSyn+ signaal doorheen de geïnjecteerde hemisfeer (Fig. 5C), wat aantoont dat het transgen daar tot expressie is gekomen.

De pleister verwijderingstest werd uitgevoerd elke 2 maanden na injectie om de motorische respons op een sensorimotorische stimulus te meten. Dit resulteerde in een niet-significant verschil in tijd-van-verwijdering (Fig. 6A). Als alternatieve gedragstest werd ook een cilindertest uitgevoerd elke 2 maanden, om het spontane voorpootgebruik te meten. Hierbij werd onverwacht een significante daling van motorfunctie geobserveerd worden in de GFP controlegroep (Fig. 6B; 2-way ANOVA, *p<0.05).

Verder werd de dopaminerge neurodegeneratie gemeten in de SN, met behulp van een TH kleuring en de Optical Fractionator tool in StereoInvestigator. Deze TH+ cel telling gaf aan dat er een onverwachte daling was in het aantal TH+ cellen in de GFP controlegroep in de geïnjecteerde kant ten opzichte van de niet geïnjecteerde kant (Fig. 7B; 2-way ANOVA, *p<0.05). *Post-hoc* analyse toonde aan dat dit een niet-significant verschil in % celverlies was tussen de twee groepen (Fig. 7C). Alsook werd een daling in intensiteit waargenomen bij de microscopische beelden van de TH kleuring in de geïnjecteerde hemisfeer van de GFP groep (Fig. 7D-E). Deze resultaten openen de mogelijkheid dat de GFP vector mogelijks toxiciteit kan induceren.

3.2 Vector titer verdunning optimalisatiestudie

Meerdere factoren kunnen geleid hebben tot de eerder geobserveerde resultaten. We veronderstelden dat deze mogelijke toxiciteit veroorzaakt kon worden door de virale overlading. Om de effecten van verdunning te testen, werd een vector titer verdunning optimalisatiestudie uitgevoerd. Twee verdunningen (5x en 10x) werden gemaakt voor striatale stereotactische injectie van de hαSyn en GFP virale constructen in vrouwelijke Sprague-Dawley ratten (n = 4 dieren/groep).

Opnieuw werd een cilindertest uitgevoerd elke 2 weken om het spontane linkse voorpootgebruik te meten over 1 maand. Geen significante verschillen werden geobserveerd in de GFP controlegroep, wat aangeeft dat de toxiciteitsproblematiek opgelost zou kunnen zijn. Voorts werd er wel een significante daling in het linkse voorpootgebruik gemeten in de 5x verdunde hαSyn groep ten opzichte van de 5x verdunde GFP groep (Fig. 8B). Vervolgens werd dopaminerge neurodegeneratie gemeten in de SN met behulp van StereoInvestigator, waar geen significante verschillen gevonden werden (Fig. 8C). Er was wel een hoge variabiliteit, vermoedelijk te wijten aan het kleine aantal dieren dat gebruikt werd bij dit experiment en de korte tijdspanne.

We kozen ervoor om verder te gaan met de 5x verdunde virale vector titer, omdat deze de hoogste titer was die geen toxiciteit veroorzaakt in de controlegroep en die nog steeds motorische defecten kon induceren in de hαSyn groep.

3.3 Nieuw 5x verdunde virale vector model

De opbouw van het nieuwe model gebeurde met een enkele striatale stereotactische injectie van 4 µl 5x verdunde hαSyn of GFP virale constructen (6 x 10^{11} GC / ml) van vrouwelijke Sprague-Dawley ratten (n = 10 dieren / groep). Dit leidde tot een wijdverspreide transductie doorheen de geïnjecteerde hemisfeer (Fig. 9C-D).

Het spontane linkse voorpootgebruik, gemeten met een cilindertest, onthulde een trend van gedaalde motorische functie in de hαSyn groep (Fig. 9B). Om hiervan de mogelijkse onderliggende neurodegeneratie te bepalen werd een TH kleuring uitgevoerd. Via StereoInvestigator werd geen verschil in aantal TH+ cellen gemeten in de SN (Fig. 10B). Bijkomend werd ook geen daling in het % TH+ immunoreactiviteit geobserveerd in zowel de SN, als het ST (Fig. 10C-F).

Aanvullend werden andere histopathologische eigenschappen van MSA onderzocht. Aan de hand van een αSyn kleuring in de hαSyn groep werd de aanwezigheid van αSyn+ globulaire structuren waargenomen (Fig. 11), die mogelijks GCI-achtige inclusies zijn. Als laatste werd oligodendrocyt dysfunctie bepaald, aan de hand van een Luxol Fast Blue kleuring, die de myeline aantoont in weefselcoupes (Fig. 12A). Met behulp van intensiteitsvergelijking van de kleuring tussen de hαSyn en GFP groepen via ImageJ werden geen significante verschillen waargenomen in intensiteit (Fig. 12B).

4. Discussie

We veronderstelden dat de virale vector-geïnduceerde overexpressie van hαSyn in oligodendrocyten zou leiden tot accumulatie van dit proteïne in GCIs, wat de histopathologische hoofdeigenschap is van MSA. Deze GCIs kunnen mogelijk oligodendrogliale dysfunctie induceren, waardoor deze oligodendroglia geen myeline meer kunnen produceren, en daaropvolgend nigrostriatale dopaminerge neurodegeneratie zouden uitlokken, wat zou leiden tot de motorische tekorten die geobserveerd worden bij MSA-P patiënten.

In de eerste reeks van experimenten werd een mogelijkse toxiciteit waargenomen in de GFP controlegroep. Dit werd geuit in de motorische defecten in een cilindertest (Fig. 6B), alsook de TH+ celtelling vertoonde een onverwachte daling in aantal TH+ cellen in deze GFP groep (Fig. 7B). Omwille van de wijdverspreide expressie van de transgenen (Fig. 5C), werd verondersteld dat de GFP controle vector mogelijks toxiciteit heeft veroorzaakt. Wij speculeerden dat een virale overlading bij de injectie, of een onzuiverheid van de gebruikte vectoren de mogelijke oorzaak kan zijn voor de toxiciteit.

Om die reden werd vervolgens een vector titer verdunning optimalisatiestudie uitgevoerd om te bepalen of de toxiciteit verklaard kon worden door virale overlading. Twee verdunningen (5x en 10x) werden gebruikt voor deze optimalisatiestudie. Geen significante motorische tekorten werden waargenomen in de GFP controlegroep bij de cilindertest (Fig. 8B), en geen verschillen in TH+ celtelling

werden gemeten (Fig. 8C), wat impliceert dat het toxiciteitsprobleem mogelijks opgelost is door de verdunning. Aangezien motorische tekorten waargenomen werden in de 5x verdunde hαSyn groep (Fig. 8B), en geen toxiciteit in de GFP controle groep werd geobserveerd, hebben we gekozen voor deze 5x verdunde titer om het nieuwe model te induceren.

Daaropvolgend werd het nieuw model gegenereerd met de 5x verdunde vector titer. Ondanks de wijdverspreide transductie van de transgenen (Fig. 9C-D), werden geen verschillen in motorische functie geobserveerd (Fig. 9B), alsook werden geen verschillen in TH+ celtellingen waargenomen in zowel SN als ST (Fig. 10B-C, F), wat dus in lijn staan met de afwezigheid van motorische achteruitgang. Verdere karakterisatie via een αSyn-immunokleuring toonde de aanwezigheid van GCI-achtige structuren in SN en ST aan (Fig. 11). Een kleuring voor myeline met Luxol Fast Blue kon geen significante demyelinatie aantonen (Fig. 12B). Dit kan mogelijks verklaard worden door een tijdsafhankelijk effect van ziekte inductie, waardoor de neuropathologie nog niet tot uiting is gekomen. Een andere verklaring kan zijn dat de vector titer in de hαSyn groep te laag was om effecten te veroorzaken.

5. Conclusie

De ontwikkeling van een virale vector-gebaseerde rattenmodel voor MSA-P heeft vertraging opgelopen, aangezien een onverwachte toxiciteit werd waargenomen in de GFP controlegroep. Daarom werd een vector titer verdunning optimalisatiestudie uitgevoerd, om de optimale vector titer te bepalen om ziekte te induceren zonder aspecifieke toxiciteit. De 5x verdunde vector induceerde motorische tekorten in de hαSyn groep, alsook werd met deze verdunning het toxiciteitsprobleem van de GFP groep opgelost. Aangezien dit de hoogste titer was die geen toxiciteit vertoonde, kozen we ervoor om door te gaan met deze 5x verdunning om het nieuwe rattenmodel mee op te bouwen. Echter werden geen motorische tekorten geïnduceerd, en geen dopaminerge neurodegeneratie kon geobserveerd worden in de SN en het ST. De aanwezigheid van GCI-achtige structuren werd hier wel waargenomen. Bijkomstig onderzoek is nodig om deze verder te karakteriseren, zoals bv. een proteïnase K behandeling. Ten slotte werd geen aantoonbaar verlies van oligodendrocytfunctie waargenomen. Aangezien een kleine zichtbare verandering in intensiteit waargenomen kon worden in de Luxol kleuring, zou een efficiëntere meetmethode wenselijk zijn. In conclusie, onze studie wijst erop dat overexpressie van hαSyn in oligodendrocyten in rat striatum met behulp van rAAV2/9 virale vector en een MAG promoter niet volstaat om MSA-P pathologie en symptomen te induceren binnen de gebruikte experimentele condities.

REFERENCES

1. Chiti F, Webster P, Taddei N, Clark A, Stefani M, Ramponi G, et al. Designing conditions for in vitro formation of amyloid protofilaments and fibrils. Proc Natl Acad Sci. 1999 Mar;96(7):3590–4.

2. Chiti F, Dobson CM. Protein Misfolding, Functional Amyloid, and Human Disease. Annu Rev Biochem. 2006 Jun;75(1):333–66.

3. Cohen AS, Calkins E. Electron Microscopic Observations on a Fibrous Component in Amyloid of Diverse Origins. Nature. 1959 Apr;183(4669):1202–3.

4. Iyer A, Claessens MMAE. Disruptive membrane interactions of alpha-synuclein aggregates. Biochim Biophys Acta - Proteins Proteomics. 2018 Oct;

5. Spillantini MG, Schmidt ML, Lee VM-Y, Trojanowski JQ, Jakes R, Goedert M. α-Synuclein in Lewy bodies. Nature. 1997 Aug;388(6645):839–40.

6. Spillantini MG, Crowther RA, Jakes R, Hasegawa M, Goedert M. alpha-Synuclein in filamentous inclusions of Lewy bodies from Parkinson's disease and dementia with lewy bodies. Proc Natl Acad Sci U S A. 1998 May;95(11):6469–73.

7. Polymeropoulos MH, Lavedan C, Leroy E, Ide SE, Dehejia A, Dutra A, et al. Mutation in the alpha-synuclein gene identified in families with Parkinson's disease. Science. 1997 Jun;276(5321):2045–7.

8. Grazia Spillantini M, Anthony Crowther R, Jakes R, Cairns NJ, Lantos PL, Goedert M. Filamentous α-synuclein inclusions link multiple system atrophy with Parkinson's disease and dementia with Lewy bodies. Neurosci Lett. 1998 Jul;251(3):205–8.

9. Maroteaux, L., Campanelli, J.T., Sheller RH. Synuclein: A neuron-specific protein localized to the nucleus and presynaptic nerve terminal. J Neurosci. 1988;8(8):2804–15.

10. Maroteaux L, Scheller RH. The rat brain synucleins; family of proteins transiently associated with neuronal membrane. Mol Brain Res. 1991 Oct;11(3–4):335–43.

11. Goedert M. Alpha-synuclein and neurodegenerative diseases. Nat Rev Neurosci. 2001 Jul;2(7):492–501.

12. Giasson BI, Murray I V, Trojanowski JQ, Lee VM. A hydrophobic stretch of 12 amino acid residues in the middle of alpha-synuclein is essential for filament assembly. J Biol Chem. 2001 Jan;276(4):2380–6.

13. Wakabayashi K, Matsumoto K, Takayama K, Yoshimoto M, Takahashi H. NACP, a presynaptic protein, immunoreactivity in Lewy bodies in Parkinson's disease. Neurosci Lett. 1997 Dec;239(1):45–8.

14. Iwai A, Masliah E, Yoshimoto M, Ge N, Flanagan L, Rohan de Silva H., et al. The precursor protein of non-Aβ component of Alzheimer's disease amyloid is a presynaptic protein of the central nervous system. Neuron. 1995 Feb;14(2):467–75.

15. Han H, Weinreb PH, Lansbury PT. The core Alzheimer's peptide NAC forms amyloid fibrils which seed and are seeded by beta-amyloid: is NAC a common trigger or target in neurodegenerative disease? Chem Biol. 1995 Mar;2(3):163–9.

16. Davidson WS, Jonas A, Clayton DF, George JM. Stabilization of alpha-synuclein secondary

structure upon binding to synthetic membranes. J Biol Chem. 1998 Apr;273(16):9443–9.

17. Murphy DD, Rueter SM, Trojanowski JQ, Lee VM-Y. Synucleins Are Developmentally Expressed, and α-Synuclein Regulates the Size of the Presynaptic Vesicular Pool in Primary Hippocampal Neurons. J Neurosci. 2000 May;20(9):3214–20.

18. Abeliovich A, Schmitz Y, Fariñas I, Choi-Lundberg D, Ho W-H, Castillo PE, et al. Mice Lacking α-Synuclein Display Functional Deficits in the Nigrostriatal Dopamine System. Neuron. 2000 Jan;25(1):239–52.

19. Jenco JM, Rawlingson A, Daniels B, Morris AJ. Regulation of Phospholipase D2: Selective Inhibition of Mammalian Phospholipase D Isoenzymes by α- and β-Synucleins †. Biochemistry. 1998 Apr;37(14):4901–9.

20. Pronin AN, Morris AJ, Surguchov A, Benovic JL. Synucleins Are a Novel Class of Substrates for G Protein-coupled Receptor Kinases. J Biol Chem. 2000 Aug;275(34):26515–22.

21. Okochi M, Walter J, Koyama A, Nakajo S, Baba M, Iwatsubo T, et al. Constitutive phosphorylation of the Parkinson's disease associated alpha-synuclein. J Biol Chem. 2000 Jan;275(1):390–7.

22. Fujiwara H, Hasegawa M, Dohmae N, Kawashima A, Masliah E, Goldberg MS, et al. α-Synuclein is phosphorylated in synucleinopathy lesions. Nat Cell Biol. 2002 Feb;4(2):160–4.

23. Gorbatyuk OS, Li S, Sullivan LF, Chen W, Kondrikova G, Manfredsson FP, et al. The phosphorylation state of Ser-129 in human alpha-synuclein determines neurodegeneration in a rat model of Parkinson disease. Proc Natl Acad Sci. 2008 Jan;105(2):763–8.

24. Richter-Landsberg C, Gorath M, Trojanowski JQ, Lee VM-Y. Alpha-synuclein is developmentally expressed in cultured rat brain oligodendrocytes. J Neurosci Res. 2000 Oct;62(1):9–14.

25. Tsuboi K, Grzesiak JJ, Bouvet M, Hashimoto M, Masliah E, Shults CW. Alpha-synuclein overexpression in oligodendrocytic cells results in impaired adhesion to fibronectin and cell death. Mol Cell Neurosci. 2005 Jun;29(2):259–68.

26. Asi YT, Simpson JE, Heath PR, Wharton SB, Lees AJ, Revesz T, et al. Alpha-synuclein mRNA expression in oligodendrocytes in MSA. Glia. 2014 Jun;62(6):964–70.

27. Miller DW, Johnson JM, Solano SM, Hollingsworth ZR, Standaert DG, Young AB. Absence of α-synuclein mRNA expression in normal and multiple system atrophy oligodendroglia. J Neural Transm. 2005 Dec;112(12):1613–24.

28. Reyes JF, Rey NL, Bousset L, Melki R, Brundin P, Angot E. Alpha-synuclein transfers from neurons to oligodendrocytes. Glia. 2014 Mar;62(3):387–98.

29. Peng C, Gathagan RJ, Covell DJ, Medellin C, Stieber A, Robinson JL, et al. Cellular milieu imparts distinct pathological α-synuclein strains in α-synucleinopathies. Nature. 2018 May;557(7706):558–63.

30. Weinreb PH, Zhen W, Poon AW, Conway KA, Lansbury PT. NACP, A Protein Implicated in Alzheimer's Disease and Learning, Is Natively Unfolded. Biochemistry. 1996 Jan;35(43):13709–15.

31. Uversky VN, Li J, Fink AL. Evidence for a partially folded intermediate in alpha-synuclein fibril formation. J Biol Chem. 2001 Apr;276(14):10737–44.

32. Adamcik J, Mezzenga R. Amyloid Polymorphism in the Protein Folding and Aggregation Energy Landscape. Angew Chemie Int Ed. 2018 Jul;57(28):8370–82.

33. Baldwin AJ, Knowles TPJ, Tartaglia GG, Fitzpatrick AW, Devlin GL, Shammas SL, et al. Metastability of Native Proteins and the Phenomenon of Amyloid Formation. J Am Chem Soc. 2011 Sep;133(36):14160–3.

34. Chiti F, Taddei N, Baroni F, Capanni C, Stefani M, Ramponi G, et al. Kinetic partitioning of protein folding and aggregation. Nat Struct Biol. 2002 Feb;9(2):137–43.

35. Giasson BI, Lee VM. Parkin and the molecular pathways of Parkinson's disease. Neuron. 2001 Sep;31(6):885–8.

36. Kordower JH, Chu Y, Hauser RA, Freeman TB, Olanow CW. Lewy body–like pathology in long-term embryonic nigral transplants in Parkinson's disease. Nat Med. 2008 May;14(5):504–6.

37. Li J-Y, Englund E, Holton JL, Soulet D, Hagell P, Lees AJ, et al. Lewy bodies in grafted neurons in subjects with Parkinson's disease suggest host-to-graft disease propagation. Nat Med. 2008 May;14(5):501–3.

38. Prusiner SB. Prions. Proc Natl Acad Sci U S A. 1998 Nov;95(23):13363–83.

39. Recasens A, Dehay B. Alpha-synuclein spreading in Parkinson's disease. Front Neuroanat. 2014 Dec;8:159.

40. Bernis ME, Babila JT, Breid S, Wüsten KA, Wüllner U, Tamgüney G. Prion-like propagation of human brain-derived alpha-synuclein in transgenic mice expressing human wild-type alpha-synuclein. Acta Neuropathol Commun. 2015 Nov;3:75.

41. Telling GC, Scott M, Hsiao KK, Foster D, Yang SL, Torchia M, et al. Transmission of Creutzfeldt-Jakob disease from humans to transgenic mice expressing chimeric human-mouse prion protein. Proc Natl Acad Sci U S A. 1994 Oct;91(21):9936–40.

42. Surmeier DJ, Obeso JA, Halliday GM. Parkinson's Disease Is Not Simply a Prion Disorder. J Neurosci. 2017;37(41):9799.

43. Bousset L, Pieri L, Ruiz-Arlandis G, Gath J, Jensen PH, Habenstein B, et al. Structural and functional characterization of two alpha-synuclein strains. Nat Commun. 2013;4:2575.

44. Trojanowski JQ, Lee VM-Y. Parkinson's Disease and Related α-Synucleinopathies Are Brain Amyloidoses. Ann N Y Acad Sci. 2006 Jan;991(1):107–10.

45. Van der Perren A, Van den Haute C, Baekelandt V. Viral Vector-Based Models of Parkinson's Disease. In Springer, Berlin, Heidelberg; 2014. p. 271–301.

46. Wirdefeldt K, Adami H-O, Cole P, Trichopoulos D, Mandel J. Epidemiology and etiology of Parkinson's disease: a review of the evidence. Eur J Epidemiol. 2011 Jun;26(S1):1–58.

47. Dauer W, Przedborski S. Parkinson's Disease: Mechanisms and Models. Neuron. 2003 Sep;39(6):889–909.

48. Kessler C, Atasu B, Hanagasi H, Simón-Sánchez J, Hauser A-K, Pak M, et al. Role of LRRK2 and SNCA in autosomal dominant Parkinson's disease in Turkey. Parkinsonism Relat Disord. 2018 Mar;48:34–9.

49. Clarimón J, Kulisevsky J. Parkinson's disease: from genetics to clinical practice. Curr Genomics. 2013 Dec;14(8):560–7.

50. Puschmann A. New Genes Causing Hereditary Parkinson's Disease or Parkinsonism. Curr Neurol Neurosci Rep. 2017 Sep;17(9):66.

51. McKeith I, Mintzer J, Aarsland D, Burn D, Chiu H, Cohen-Mansfield J, et al. Dementia with

Lewy bodies. Lancet Neurol. 2004 Jan;3(1):19–28.

52. Savica R, Grossardt BR, Bower JH, Boeve BF, Ahlskog JE, Rocca WA. Incidence of Dementia With Lewy Bodies and Parkinson Disease Dementia. JAMA Neurol. 2013 Nov;70(11):1396.

53. Goodman RA, Lochner KA, Thambisetty M, Wingo TS, Posner SF, Ling SM. Prevalence of dementia subtypes in United States Medicare fee-for-service beneficiaries, 2011-2013. Alzheimers Dement. 2017;13(1):28–37.

54. Richard IH, Papka M, Rubio A, Kurlan R. Parkinson's disease and dementia with Lewy bodies: One disease or two? Mov Disord. 2002 Nov;17(6):1161–5.

55. Quinn N. Multiple system atrophy--the nature of the beast. J Neurol Neurosurg Psychiatry. 1989 Jun;Suppl(Suppl):78–89.

56. Watanabe H, Saito Y, Terao S, Ando T, Kachi T, Mukai E, et al. Progression and prognosis in multiple system atrophy. Brain. 2002 May;125(5):1070–83.

57. Gilman S, Low P, Quinn N, Albanese A, Ben-Shlomo Y, Fowler C, et al. Consensus statement on the diagnosis of multiple system atrophy. American Autonomic Society and American Academy of Neurology. Clin Auton Res. 1998 Dec;8(6):359–62.

58. Schrag A, Ben-Shlomo Y, Quinn N. Prevalence of progressive supranuclear palsy and multiple system atrophy: a cross-sectional study. Lancet. 1999 Nov;354(9192):1771–5.

59. Tison F, Yekhlef F, Chrysostome V, Sourgen C. Prevalence of multiple system atrophy. Lancet (London, England). 2000 Feb;355(9202):495–6.

60. Graham JG, Oppenheimer DR. Orthostatic hypotension and nicotine sensitivity in a case of multiple system atrophy. J Neurol Neurosurg Psychiatry. 1969 Feb;32(1):28–34.

61. Ozawa T, Onodera O. Multiple system atrophy: clinicopathological characteristics in Japanese patients. Proc Japan Acad Ser B. 2017;93(5):251–8.

62. Gilman S. Parkinsonian Syndromes. Clin Geriatr Med. 2006 Nov;22(4):827–42.

63. Wenning GK, Ben Shlomo Y, Magalhães M, Daniel SE, Quinn NP. Clinical features and natural history of multiple system atrophy. An analysis of 100 cases. Brain. 1994 Aug;117 (Pt 4):835–45.

64. Papp MI, Kahn JE, Lantos PL. Glial cytoplasmic inclusions in the CNS of patients with multiple system atrophy (striatonigral degeneration, olivopontocerebellar atrophy and Shy-Drager syndrome). J Neurol Sci. 1989 Dec;94(1–3):79–100.

65. Wakabayashi K, Yoshimoto M, Tsuji S, Takahashi H. Alpha-synuclein immunoreactivity in glial cytoplasmic inclusions in multiple system atrophy. Neurosci Lett. 1998 Jun;249(2–3):180–2.

66. Tu P, Galvin JE, Baba M, Giasson B, Tomita T, Leight S, et al. Glial cytoplasmic inclusions in white matter oligodendrocytes of multiple system atrophy brains contain insoluble ?-synuclein. Ann Neurol. 1998 Sep;44(3):415–22.

67. Nakazato Y, Yamazaki H, Hirato J, Ishida Y, Yamaguchi H. Oligodendroglial microtubular tangles in olivopontocerebellar atrophy. J Neuropathol Exp Neurol. 1990 Sep;49(5):521–30.

68. Wenning GK, Jellinger KA. The role of alpha-synuclein in the pathogenesis of multiple system atrophy. Acta Neuropathol. 2005 Feb;109(2):129–40.

69. Dickson DW. Parkinson's disease and parkinsonism: neuropathology. Cold Spring Harb Perspect Med. 2012 Aug;2(8):a009258.

70. Baumann N, Pham-Dinh D. Biology of Oligodendrocyte and Myelin in the Mammalian Central Nervous System. Physiol Rev. 2001 Apr;81(2):871–927.

71. Wüllner U, Abele M, Schmitz-Huebsch T, Wilhelm K, Benecke R, Deuschl G, et al. Probable multiple system atrophy in a German family. J Neurol Neurosurg Psychiatry. 2004 Jun;75(6):924–5.

72. Soma H, Yabe I, Takei A, Fujiki N, Yanagihara T, Sasaki H. Heredity in multiple system atrophy. J Neurol Sci. 2006 Jan;240(1–2):107–10.

73. Hara K, Momose Y, Tokiguchi S, Shimohata M, Terajima K, Onodera O, et al. Multiplex Families With Multiple System Atrophy. Arch Neurol. 2007 Apr;64(4):545.

74. Multiple-System Atrophy Research Collaboration. Mutations in *COQ2* in Familial and Sporadic Multiple-System Atrophy. N Engl J Med. 2013 Jul;369(3):233–44.

75. Ozawa T, Takano H, Onodera O, Kobayashi H, Ikeuchi T, Koide R, et al. No mutation in the entire coding region of the α-synuclein gene in pathologically confirmed cases of multiple system atrophy. Neurosci Lett. 1999 Jul;270(2):110–2.

76. Beal MF. Mitochondria, Oxidative Damage, and Inflammation in Parkinson's Disease. Ann N Y Acad Sci. 2006 Jan;991(1):120–31.

77. Fernagut P-O, Ghorayeb I, Diguet E, Tison F. In vivo models of multiple system atrophy. Mov Disord. 2005 Aug;20(S12):S57–63.

78. Ungerstedt U, Arbuthnott GW. Quantitative recording of rotational behavior in rats after 6-hydroxy-dopamine lesions of the nigrostriatal dopamine system. Brain Res. 1970 Dec;24(3):485–93.

79. Sauer H, Oertel WH. Progressive degeneration of nigrostriatal dopamine neurons following intrastriatal terminal lesions with 6-hydroxydopamine: A combined retrograde tracing and immunocytochemical study in the rat. Neuroscience. 1994 Mar;59(2):401–15.

80. Wenning GK, Granata R, Laboyrie PM, Quinn NP, Jenner P, Marsden CD. Reversal of behavioural abnormalities by fetal allografts in a novel rat model of striatonigral degeneration. Mov Disord. 1996 Sep;11(5):522–32.

81. Kaindlstorfer C, García J, Winkler C, Wenning GK, Nikkhah G, Döbrössy MD. Behavioral and histological analysis of a partial double-lesion model of parkinson-variant multiple system atrophy. J Neurosci Res. 2012 Jun;90(6):1284–95.

82. Langston JW, Irwin I, Langston EB, Forno LS. 1-Methyl-4-phenylpyridinium ion (MPP+): identification of a metabolite of MPTP, a toxin selective to the substantia nigra. Neurosci Lett. 1984 Jul;48(1):87–92.

83. Ghorayeb I, Fernagut P., Hervier L, Labattu B, Bioulac B, Tison F. A 'single toxin–double lesion' rat model of striatonigral degeneration by intrastriatal 1-methyl-4-phenylpyridinium ion injection: a motor behavioural analysis. Neuroscience. 2002 Dec;115(2):533–46.

84. Heikkila RE, Manzino L, Cabbat FS, Duvoisin RC. Protection against the dopaminergic neurotoxicity of 1-methyl-4-phenyl-1,2, 5,6-tetrahydropyridine by monoamine oxidase inhibitors. Nature. 1984;311(5985):467–9.

85. Shen RS, Abell CW, Gessner W, Brossi A. Serotonergic conversion of MPTP and dopaminergic accumulation of MPP+. FEBS Lett. 1985 Sep;189(2):225–30.

86. Becker K, Wang X, Vander Stel K, Chu Y, Kordower J, Ma J. Detecting Alpha Synuclein Seeding

Activity in Formaldehyde-Fixed MSA Patient Tissue by PMCA. Mol Neurobiol. 2018 Nov;55(11):8728–37.

87. Watts JC, Giles K, Oehler A, Middleton L, Dexter DT, Gentleman SM, et al. Transmission of multiple system atrophy prions to transgenic mice. Proc Natl Acad Sci U S A. 2013 Nov;110(48):19555–60.

88. Polinski NK, Volpicelli-Daley LA, Sortwell CE, Luk KC, Cremades N, Gottler LM, et al. Best Practices for Generating and Using Alpha-Synuclein Pre-Formed Fibrils to Model Parkinson's Disease in Rodents. J Parkinsons Dis. 2018;8(2):303–22.

89. Luk KC, Kehm V, Carroll J, Zhang B, O'Brien P, Trojanowski JQ, et al. Pathological α-synuclein transmission initiates Parkinson-like neurodegeneration in nontransgenic mice. Science. 2012 Nov;338(6109):949–53.

90. Luk KC, Kehm VM, Zhang B, O'Brien P, Trojanowski JQ, Lee VMY. Intracerebral inoculation of pathological α-synuclein initiates a rapidly progressive neurodegenerative α-synucleinopathy in mice. J Exp Med. 2012 May;209(5):975–86.

91. Palmiter RD, Brinster RL, Hammer RE, Trumbauer ME, Rosenfeld MG, Birnberg NC, et al. Dramatic growth of mice that develop from eggs microinjected with metallothionein-growth hormone fusion genes. Nature. 1982 Dec;300(5893):611–5.

92. Kahle PJ, Neumann M, Ozmen L, Muller V, Jacobsen H, Spooren W, et al. Hyperphosphorylation and insolubility of alpha-synuclein in transgenic mouse oligodendrocytes. EMBO Rep. 2002 Jun;3(6):583–8.

93. Yazawa I, Giasson BI, Sasaki R, Zhang B, Joyce S, Uryu K, et al. Mouse Model of Multiple System Atrophy α-Synuclein Expression in Oligodendrocytes Causes Glial and Neuronal Degeneration. Neuron. 2005 Mar;45(6):847–59.

94. Shults CW, Rockenstein E, Crews L, Adame A, Mante M, Larrea G, et al. Neurological and Neurodegenerative Alterations in a Transgenic Mouse Model Expressing Human -Synuclein under Oligodendrocyte Promoter: Implications for Multiple System Atrophy. J Neurosci. 2005 Nov;25(46):10689–99.

95. Srivastava A, Lusby EW, Berns KI. Nucleotide sequence and organization of the adeno-associated virus 2 genome. J Virol. 1983 Feb;45(2):555–64.

96. Hermonat PL, Muzyczka N. Use of adeno-associated virus as a mammalian DNA cloning vector: transduction of neomycin resistance into mammalian tissue culture cells. Proc Natl Acad Sci U S A. 1984 Oct;81(20):6466–70.

97. Dong B, Nakai H, Xiao W. Characterization of genome integrity for oversized recombinant AAV vector. Mol Ther. 2010 Jan;18(1):87–92.

98. Samulski RJ, Muzyczka N. AAV-Mediated Gene Therapy for Research and Therapeutic Purposes. Annu Rev Virol. 2014 Nov;1(1):427–51.

99. Louis Jeune V, Joergensen JA, Hajjar RJ, Weber T. Pre-existing anti-adeno-associated virus antibodies as a challenge in AAV gene therapy. Hum Gene Ther Methods. 2013 Apr;24(2):59–67.

100. Dong J-Y, Fan P-D, Frizzell RA. Quantitative Analysis of the Packaging Capacity of Recombinant Adeno-Associated Virus. Hum Gene Ther. 1996 Nov;7(17):2101–12.

101. Castle MJ, Turunen HT, Vandenberghe LH, Wolfe JH. Controlling AAV Tropism in the Nervous System with Natural and Engineered Capsids. Methods Mol Biol. 2016;1382:133–49.

102. Gow A, Friedrich VL, Lazzarini RA. Myelin basic protein gene contains separate enhancers for oligodendrocyte and Schwann cell expression. J Cell Biol. 1992 Nov;119(3):605–16.

103. Bassil F, Guerin PA, Dutheil N, Li Q, Klugmann M, Meissner WG, et al. Viral-mediated oligodendroglial alpha-synuclein expression models multiple system atrophy. Mov Disord. 2017 Aug;32(8):1230–9.

104. Martini R, Schachner M. Molecular bases of myelin formation as revealed by investigations on mice deficient in glial cell surface molecules. Glia. 1997 Apr;19(4):298–310.

105. von Jonquieres G, Fröhlich D, Klugmann CB, Wen X, Harasta AE, Ramkumar R, et al. Recombinant Human Myelin-Associated Glycoprotein Promoter Drives Selective AAV-Mediated Transgene Expression in Oligodendrocytes. Front Mol Neurosci. 2016;9:13.

106. Van der Perren A, Toelen J, Carlon M, Van den Haute C, Coun F, Heeman B, et al. Efficient and stable transduction of dopaminergic neurons in rat substantia nigra by rAAV 2/1, 2/2, 2/5, 2/6.2, 2/7, 2/8 and 2/9. Gene Ther. 2011 May;18(5):517–27.

107. Bassil F, Guerin PA, Dutheil N, Li Q, Klugmann M, Meissner WG, et al. Viral-mediated oligodendroglial alpha-synuclein expression models multiple system atrophy. Mov Disord. 2017 Aug;32(8):1230–9.

108. Schallert T, Fleming SM, Leasure JL, Tillerson JL, Bland ST. CNS plasticity and assessment of forelimb sensorimotor outcome in unilateral rat models of stroke, cortical ablation, parkinsonism and spinal cord injury. Neuropharmacology. 2000 Apr;39(5):777–87.

109. Kluver H, Barrera E. A method for the combined staining of cells and fibers in the nervous system. J Neuropathol Exp Neurol. 1953 Oct;12(4):400–3.

110. Watanabe H, Sobue G. A milestone on the way to therapy for MSA. Lancet Neurol. 2013 Mar;12(3):222–3.

111. Wenning GK, Stefanova N, Jellinger KA, Poewe W, Schlossmacher MG. Multiple system atrophy: A primary oligodendrogliopathy. Ann Neurol. 2008 Sep;64(3):239–46.

112. Ubhi K, Low P, Masliah E. Multiple system atrophy: a clinical and neuropathological perspective. Trends Neurosci. 2011 Nov;34(11):581–90.

113. Ozawa T, Paviour D, Quinn NP, Josephs KA, Sangha H, Kilford L, et al. The spectrum of pathological involvement of the striatonigral and olivopontocerebellar systems in multiple system atrophy: clinicopathological correlations. Brain. 2004 Nov;127(12):2657–71.

114. Sato K, Kaji R, Matsumoto S, Nagahiro S, Goto S. Compartmental loss of striatal medium spiny neurons in multiple system atrophy of parkinsonian type. Mov Disord. 2007 Sep;22(16):2365–70.

115. Gerfen CR. The neostriatal mosaic: compartmentalization of corticostriatal input and striatonigral output systems. Nature. 311(5985):461–4.

116. Smith JB, Klug JR, Ross DL, Howard CD, Hollon NG, Ko VI, et al. Genetic-Based Dissection Unveils the Inputs and Outputs of Striatal Patch and Matrix Compartments. Neuron. 2016 Sep;91(5):1069–84.

117. Schwarz L, Goldbaum O, Bergmann M, Probst-Cousin S, Richter-Landsberg C. Involvement of Macroautophagy in Multiple System Atrophy and Protein Aggregate Formation in Oligodendrocytes. J Mol Neurosci. 2012 Jun;47(2):256–66.

118. Ubhi K, Rockenstein E, Mante M, Inglis C, Adame A, Patrick C, et al. Neurodegeneration in a

Transgenic Mouse Model of Multiple System Atrophy Is Associated with Altered Expression of Oligodendroglial-Derived Neurotrophic Factors. J Neurosci. 2010 May;30(18):6236–46.

119. Stefanova N, Kaufmann WA, Humpel C, Poewe W, Wenning GK. Systemic proteasome inhibition triggers neurodegeneration in a transgenic mouse model expressing human α-synuclein under oligodendrocyte promoter: implications for multiple system atrophy. Acta Neuropathol. 2012 Jul;124(1):51–65.

120. Don AS, Hsiao J-HT, Bleasel JM, Couttas TA, Halliday GM, Kim WS. Altered lipid levels provide evidence for myelin dysfunction in multiple system atrophy. Acta Neuropathol Commun. 2014 Oct;2:150.

121. Mandel RJ, Marmion DJ, Kirik D, Chu Y, Heindel C, McCown T, et al. Novel oligodendroglial alpha synuclein viral vector models of multiple system atrophy: studies in rodents and nonhuman primates. Acta Neuropathol Commun. 2017;5(1):47.

122. Deverman BE, Pravdo PL, Simpson BP, Kumar SR, Chan KY, Banerjee A, et al. Cre-dependent selection yields AAV variants for widespread gene transfer to the adult brain. Nat Biotechnol. 2016 Feb;34(2):204–9.